# PERFORMANCE ASSESSMENT OF SOLAR DRYER INTEGRATED WITH HEAT ENERGY STORAGE SYSTEM FOR FOOD PRESERVATION

**Wenceslaus Pantaleo Missana**

**A Dissertation Submitted in Partial Fulfilment of the Requirements for the Degree of Master's in Sustainable Energy Science and Engineering of the Nelson Mandela African Institution of Science and Technology**

**Arusha, Tanzania**

**January, 2022**

# ABSTRACT

Solar energy is regarded as a clean form of energy because solar radiation can be transformed into heat energy for different applications such as heating water, generating power, cooking, and drying food products. The solar dryer integrated with heat energy storage system in this study was designed to use nitrate salt as a phase change material that can store thermal energy during sun hours and then be used when the sun is not active. The dryer was tested by drying 1000 g of red peppers in a drying air temperature range of 19.6 – 62.4 °C, the average temperature was 46 °C and ambient temperature ranges between 19.3 – 37.4 °C. The drying process of the developed solar dryer was compared with an open sun drying system, each loaded with 1000 g of red pepper. For 24 hours, the solar dryer maintained colour, flavor and reduced the moisture content from 86% to the required 10% whereas open sun drying took 36 hours to accomplish the same result. It has been discovered that the payback period is 6.2 years, which is low compared to the 22-year solar dryer life span. Thus, for 16 years, the solar dryer will dry free products, which is feasible and economical.

# DECLARATION

I, Wenceslaus Pantaleo Missana, do hereby declare to the Senate of the Nelson Mandela African Institution of Science and Technology that this dissertation is my own original work and that it has neither been submitted nor being concurrently submitted for degree award in any other institution.

Wenceslaus Pantaleo Missana

Name and Signature of Candidate Date

The above declaration is confirmed by:

Dr. Thomas T. Kivevele

Name and Signature of Candidate Date

Prof. Eugene Park

Name of Supervisor 1 Date

# COPYRIGHT

# CERTIFICATION

The undersigned certify that have read and hereby recommend for acceptance by the Nelson Mandela Institution of Science and Technology a dissertation titled *“Performance Assessment of Solar Dryer Integrated with Heat Energy Storage System for Food Preservation”* In Partial Fulfilment of the Requirements for the Degree of Master’s in Sustainable Energy Science and Engineering of the Nelson Mandela African Institution of Science and Technology.

Dr. Thomas T. Kivevele

Name and Signature of Candidate Date

Prof. Eugene Park

Name of Supervisor 1 Date

# ACKNOWLEDGEMENTS

I would like to acknowledge and express my sincere thanks to the Nelson Mandela African Institution of Science and Technology for allowing me to join this program. I also thank my employer, the Arusha Technical College for granting me study leave and the Board of Loans for Higher Education Students for providing a loan to cover my study costs through my employer. I am also grateful to the Centre for Agricultural Mechanization and Rural Technology (CAMARTEC) for helping me with fundamental data on passive solar dryers and modification of the dryer design. Finally, I appreciate the assistance and encouragements of my supervisors: Dr. Thomas T. Kivevele and Prof. Eugene Park, my family and friends during the period of undertaking of studies.

# DEDICATION

This research work is dedicated to my late parents, Mr. and Mrs. P E Missana, who raised me with love and care "Rest your soul in peace".

## TABLE OF CONTENTS

## LIST OF TABLES

# LIST OF FIGURES

# LIST OF APPENDICES

# LIST OF ABBREVIATIONS AND SYMBOLS

| | |
|---|---|
| $\Delta T$ | Change in Temperature (°) |
| A | Area ($m^2$) |
| $A_c$ | Area of Collector ($m^2$) |
| ATC | Arusha Technical College |
| c | Collector |
| CAC | Codex Alimentarius Commission |
| CARMATEC | Centre for Agricultural Mechanization and Rural Technology |
| CFD Simulation | Computational Fluid Dynamics Simulation Software |
| $Cp_a$ | Specific Heat Capacity of Air (kJ/kg K) |
| $CR_g$ | Geometric Concentration Ratio |
| $D_a$ | Aperture Diameter (m) |
| DR | Drying Rate (kg of water / kg of dry matter per hour) |
| E | Energy (J) |
| e | Equilibrium |
| F | Focal Length (m) |
| f | Final |
| H | Depth of Parabola (m) |
| HSM | Heat Storage Material |
| I | Solar Intensity (W/ $m^2$) |
| i | Initial |
| $KNO_3$ | Potassium Nitrate |
| LPG Burners | Liquefied Petroleum Gas Burners |
| M | Mass of Product (kg) |
| $M_a$ | Mass Flow Rate of Air (kg/s) |
| MC | Moisture Content (%) |
| MEWES | Materials, Energy, Water, and Environmental Sciences |
| MR | Moisture Ratio |
| $NaNO_3$ | Sodium Nitrate |
| NM-AIST | Nelson Mandela African Institution of Science and Technology |
| PCM | Phase Change Material |
| PTC | Parabolic Trough Collector |

| | |
|---|---|
| PV | Photovoltaic |
| S | Arc Length of the Parabolic Curve (m) |
| SD | Solar Dish |
| SDIHESS | Solar Dryer Integrated with Heat Energy Storage System |
| T | Temperature (°C) |
| t | Drying Time (hour) |
| TZS | Tanzanian Shillings |
| W | Velocity (m/s) |
| w | Wet Basis |
| $W_{Hr}$ | Relative Humidity |
| $W_M$ | Weight |
| $W_S$ | Solar Radiation Intensity |
| $W_{Ta}$ | Ambient Temperature |
| $W_{Tc}$ | Drying Temperature |
| $W_{Th}$ | Heat Storage Material Temperature |
| $W_V$ | Air Velocity |
| $\alpha$ | Absorptivity |
| $\beta$ | Angle of Inclination (°) |
| $\eta$ | Efficiency (%) |
| $\rho_a$ | Density of Air ($kg/m^3$) |
| $\tau$ | Transmissivity |
| $\phi$ | Latitude (°) |
| $\psi$ | Angle of Reflection (°) |

# CHAPTER ONE

# INTRODUCTION

## 1.1 Background of the Problem

Renewable energy is an energy source that is constantly replenished by nature which are derived from the sun, natural movements or environmental mechanism. Solar, hydropower, biomass, wind, geothermal and tidal energy are examples of renewable energy resources (Ellabban *et al.*, 2014). Solar energy is more abundant that transforms sunlight into other power. Solar photovoltaic (PV) converts solar energy into electricity by means of photoelectric effects while solar thermal energy transforms solar radiation into heat energy for different purposes such as heating water, space heating /air conditioning, power generation, cooking, drying food and crops (Pankaew *et al.*, 2020).

The use of solar energy for drying vegetables, crops, fruits, plants and other biomaterials has practice in many areas and proved to be economical and environmentally friendly. Solar drying techniques are the traditional way of drying agricultural produce. In the African continent, almost 40% of agricultural products, especially food products are being lost through spoilage (Suleiman & Kurt, 2015). The reasons are poor ways of preservation, inadequate transportation systems and the low price for the products in the rural markets. Thus, in Tanzania, the use of simple passive solar dryers to dry agricultural products is an economic way. Open sun and controlled sun drying are common systems of drying. Open sun drying is a traditional method of preserving food by laying products in the sun on mattresses, roofs or drying floors and it is a cheap way of drying. However, it can spoil the product due to dust, dirt, fungus, bacterium and animal attack (Lingayat *et al.*, 2020). Controlled drying involves the use of passive and active solar dryers (Hussein *et al.*, 2017). The passive solar dryer (natural convection) is used for drying crops or food products and is widely used because it is a cheap technology. The active solar dryer (forced convection) is an efficient solar dryer used in small firms for dry food or other products for a short period, however, the technology is still expensive for peasant (Mustayen *et al.*, 2014). Different designs of passive solar dryers for drying crops and food products have been developed in Tanzania. The Centre for Agricultural Mechanization and Rural Technology (CARMATEC – Arusha) has designed three types of passive solar dryers i.e. (direct, indirect and mixed mode) as shown Fig. 1. However, these designs were not in accordance with the Codex Alimentarius Commission (CAC) which is responsible for formulating the standards, codes of practice, guidelines and recommendations for protecting the health of consumers and ensuring the fair practice in the food trade (Comission, 2003). In addition, the dryers are purely passive and solely depend on the presence of solar radiation for drying of crops and food products and turn into useless devices in the absence of solar radiation. Thus, introducing a heat storage system to the developed dryers is imperative. The integration of heat storage enables heat collection during sunlight for later use, hence increase productivity (Mongi *et al.*, 2015). The passive solar dryers developed by the Centre for Agricultural Mechanization and Rural Technology are shown in Fig. 1.


**Figure 1: CARMATEC Dryers; Direct (A), Indirect (B), Mixed-mode (C) (Centre for Agricultural Mechanization and Rural Technology [CARMATEC], 2018)**

Table 1: shows some recommended drying temperatures for food products as described by Scanlin (1997).

**Table 1: Recommended drying temperatures**

| S/No. | Food products | Temperature |
|---|---|---|
| 1. | Fruits and vegetables | 37.8 - 60°C |
| 2. | Meat | 60 - 65.6°C |
| 3. | Fish | 60 - 65.6°c |
| 4. | Herbs | 35 - 40.6°C |
| 5. | Rice, Grains, Seeds, Brewery Grains | 45°C Maximum temperature |
| 6. | Livestock feed | 75°C Maximum temperature |

**Scanlin (1997)**

## 1.2 Statement of the Problem

Open sun and controlled sun drying are common systems of drying. Different designs of passive solar dryers for drying crops and food products have been developed in Tanzania. For instance, the Centre for Agricultural Mechanization and Rural Technology (CARMATEC –

Arusha) has designed three types of passive solar dryers i.e. (direct, indirect and mixed mode) as shown Fig. 1. However, these designs were not in accordance with the Codex Alimentarius Commission (CAC) which is responsible for formulating the standards, codes of practice, guidelines and recommendations for protecting the health of consumers and ensuring the fair practice in the food trade (Comission, 2003). In addition, the dryers are purely passive and solely depend on the presence of solar radiation for drying of crops and food products and turn into useless devices in the absence of solar radiation. Thus, introducing a heat storage system to the developed dryers is imperative. The integration of heat storage enables heat collection during sunlight for later use, hence increase productivity (Mongi *et al.*, 2015). Therefore, the purpose of this study is to evaluate the effectiveness of the solar dryer integrated with the heat storage system. A nitrate salt was selected as a heat storage medium because after studied the comprehensive literature review was shown to have the good temperature reached above 100°C, although nitrate salt was used in the solar cookers, but it has not been used for solar dryer.

## 1.3 Rationale of the Study

Open sun drying is a traditional method of preserving food by laying products in the sun on mattresses, roofs or drying floors and it is a cheap way of drying. However, it can spoil the product due to dust, dirt, fungus, bacterium and animal attack (Lingayat *et al.*, 2020). In the African continent, almost 40% of agricultural products, especially food products are being lost through spoilage (Suleiman & Kurt, 2015). The reasons are poor ways of preservation, inadequate transportation systems and the low price for the products in the rural markets. Thus, in Tanzania, the use of simple passive solar dryers to dry agricultural products is an economic way. Therefore, based on this, a new way of drying particularly agricultural products, which is environmental friendly, capable of ensuring food safety aspects and affordable to ordinary peasant is necessary. Different designs of passive solar dryers for drying crops and food products have been developed in Tanzania. However, these designs were not in accordance with the Codex Alimentarius Commission (CAC). In addition, the dryers are purely passive and solely depend on the presence of solar radiation for drying of crops and food products and turn into useless devices in the absence of solar radiation. Thus, introducing a heat storage system to the developed dryers is imperative.

## 1.4 Research Objectives

### 1.4.1 General Objective

The main objective of the present study is to design and evaluate the performance of the solar dryer integrated with a heat storage system that uses nitrate salt as a storage media for food preservation.

### 1.4.2 Specific Objectives

The specific objectives of this research are as follows:

(i) To design solar dryer integrated with heat energy storage system.

(ii) To develop solar dryer integrated with heat energy storage system.

(iii) To investigate the performance of solar dryer integrated with heat energy storage system.

(iv) To investigate the economic feasibility of the solar dryer integrated with heat storage system.

## 1.5 Research Questions

(i) What is the design for solar dryer integrated with heat energy storage system?

(ii) How will solar dryer be integrated with heat storage system?

(iii) How is the solar dryer integrated with heat storage system function?

(iv) What is the the economic feasibility of the solar dryer integrated with heat storage system?

## 1.6 Hypothesis

The main hypothesis of this study is that a low-cost and efficient solar dryer integrated with a heat storage system using nitrate salt as a storage medium achieves good drying performance and provides high-quality dried products in terms of appearance, aroma, and texture. The hypothesis is tested by various experiments such as measurements of temperatures, relative humidity, solar intensity, drying rate and air velocity.

## 1.7 Significance of the Study

More than 80 percent of Tanzanian lives in the rural areas where are engaged in farming and fishing (Blomley & Ramadhani, 2006). Also, Tanzanian is producing a total of more than 142 types of processes food per year (Tomar *et al.*, 2017). The improper methods of food drying forced the majority to throw their products like tomatoes, potatoes, fruits, vegetables, fish and meat after spoiling (Lingayat *et al.*, 2017). Solar drying systems can improve the quality and reducing waste of food products. The importance of this study is to support the societies by introducing the solar dryer, integrated with heat energy storage system which will be capable to store heat energy for later use and reduce the problem of the food spoilage (postharvest loss), environmental damage, provide a better quality of food products for final consumers and increase the income of the society and self-employment.

## 1.8 Delineation of the Study

The use of solar energy for drying vegetables, crops, fruits, plants and other biomaterials has practice in many areas and proved to be economical and environmentally friendly. Solar drying techniques are the traditional way of drying agricultural produce. Therefore, the present study focused to evaluate the effectiveness of the solar dryer integrated with the heat storage system so as to outweigh the weaknesses associated with passive solar dryers.

# CHAPTER TWO

# LITERATURE REVIEW

## 2.1 Heat Storage Materials

In a latent heat storage system, heat storage materials (HSMs) are materials used to store energy, they absorbs or releases energy during the melting-solidification cycle which is known as the latent heat of fusion, they are mass-based processes measured in units of J/g or kJ/kg (Mohamed *et al.*, 2017). The choice of storage media depends on many factors, including storage duration, the temperature required, storage capacity, heat losses, economics and space available. Heat storage materials based on sensible heat, latent heat or chemical reactions involve at least three steps: Heat charging, storage and discharging to utilize thermal energy. The central receivers, parabolic trough and paraboloidal dishes via thermal and chemical conversion are techniques employed to utilize solar power as reported by Zhang *et al.* (2016).

## 2.2 Parabolic Trough Collectors

Bellos *et al.* (2016) discussed the parabolic trough collectors (PTCs) that are the most mature technology for using solar energy in high-temperature applications. The PTCs are often used for a steam generation because of their high-temperature ranges above 100°C up to 300°C or more, depending on the location, length, numbers or pieces of the parabolic trough collectors and applications. The PTC surface focuses on the solar radiation then reflects back to the absorber pipe and then transmits heat to the thermal fluid. Solar energy was concentrated on the absorber pipe to change the phase of water liquid to steam.

Conrado *et al.* (2017) studied solar collectors' thermal performance analysis, applied various mathematical models, simulation, numerical methods, and experimental setup to investigate loss of heat, temperature, heat flux and environmental conditions. Also assess cost analysis and economic strategy for PTCs. The study's objective was to demonstrate the principal thermal aspects required in the parabolic trough collectors' future developments. The general working principle of parabolic trough collectors highlights the parabola geometry as reported by Hafez *et al.* (2018). A parabolic trough collector is shown in Fig. 2.

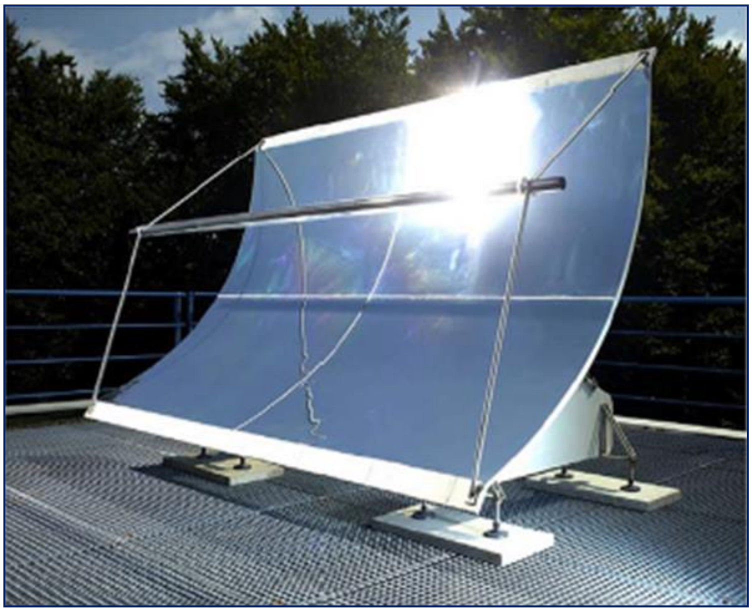

**Figure 2: Parabolic trough collector (Hafez *et al.*, 2018)**

## 2.3 Reviews and Some Related Studies

Lingayat *et al.* (2017) researched the data related to drying analysis of the passive solar dryer without loading as shown in Fig. 3. The solar radiation, ambient temperature ($T_{amb}$), collector outlet temperature ($T_{out}$) and drying chamber outlet temperature ($T_{dout}$) were assessed and plotted. The maximum solar radiation of 1219 W/m$^2$ was noted at 12.40 hours while the average solar radiation was 897.04 W/m$^2$. Likewise, for no load tests, the maximum temperature of air at the outlet of the collector and the chamber was noted as 81°C and 78°C respectively. The experiment showed, the variation of daily mean air temperature at the dryer inlet was ranged between 38°C and 81°C, the variation of solar radiations was between 192 and 1220 W/m$^2$. The study was conducted and recorded during the sunlight between March and June 2016 at National Institute of Technology (NIT) Warangal in India. The graphs of solar radiation, air temperature, relative humidity and drying time are shown in Fig. 3.

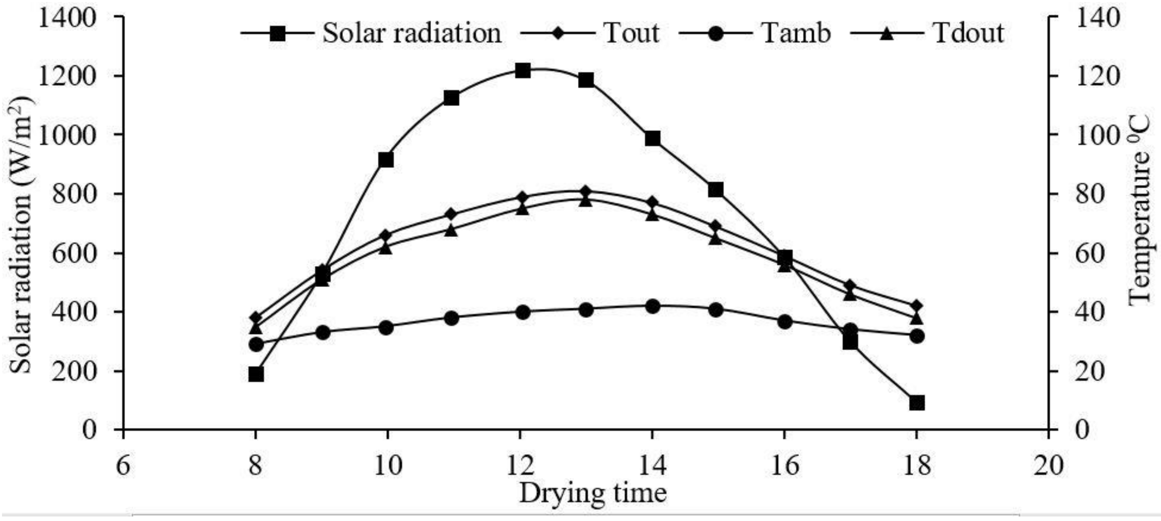


**Figure 3: Solar radiation, Air temperature, relative humidity and drying time (Lingayat *et al.*, 2017)**

Rabha and Muthukumar (2017) conducted the performance studies of the active solar dryer, integrated with a paraffin wax-based shell and tube latent heat storage unit by heating a storage material to be used for heating applications at a later time. The dryer was tested by drying 20 kg of red chill in the drying air temperature range of 36 to 60°C. During the experiment, the charging process of heat storage medium was stored in the shell and air flowed through the tube. Heat energy was transferred to the drying box through tubes with the help of a blower for the discharge process. The initial moisture content of the chili was 73.5% (w.t) and was reduced to the final moisture contents of 9.7% (w.t) in 4 consecutive days. The dryer was operated daily for 10 hours from 8:00 to 18:00 hour (h). The ambient temperature varied between 24°C and 35°C. The maximum air temperature was 70°C in their study.

Da Cunha and Eames (2016) reviewed some studies that investigated phase change materials to store heat energy for different applications and showed the thermal physical properties above 100 ºC for organic compounds and the salt hydrate materials. Other studies of eutectic mixture with urea were also tasted and showed a temperature of around 100ºC, a eutectic inorganic salt mixture ranged from 130ºC to 1250ºC, but a mixture of sodium and potassium melt around 170ºC and appears attractive in thermal storage applications.

Jain and Tewari (2015) developed a natural convective solar dryer with heat energy storage material for phase change in order to ensure continuity of the drying process. The heat storage material was stored the thermal energy during sunshine hours and released the latent heat after sunset and effectively operate the solar dryer for the next 5 - 6 hours after sunlight.

Kant *et al.* (2017) presented thermal storage materials that attracted many researchers when reviewed different studied and applications whose achieved an analysis of heat storage materials depends on the type of heat storage media. In the review concluded that, the performance of thermal energy storage system is directly associated with the phase transition properties of heat storage materials. Kalbande *et al.* (2017) discussed solar energy that transforms solar radiation intensity into heat energy to dry food and plants. Panwar *et al.* (2011) reported that, in many nations agricultural products, particularly vegetables and fruits, are lost for over 40% of postharvest through spoilage.

Chavan *et al.* (2020) discussed the open sun and controlled solar dryer and observed that, open sun drying is a conventional way to preserve food that involves putting crops on mats, roofs or drying floors in the sun and is an inexpensive way to dry out. However, due to dust, dirt, fungi, bacteria and animal attacks can spoil food products. Mawire *et al.* (2020) studied the application of sunflower oil as a heat transfer medium and a sensible heat storage material, and justified the availability in most countries in the world. The sunflower had a boiling point of 230°C and a flash point of 250°C.

Bhardwaj *et al.* (2019) investigated indirect forced convection solar dryer integrated with sensible heat storage material (SHSM) and phase change material (PCM), the scrap of iron combined with gravel and the engine oil in the solar air collector was used as SHSM and the rt-42 paraffin was used as a PCM. The drying rate for SHSM and PCM was 0.051 kg/ h, SHSM's energy and exergy efficiency was 26.1 and 0.81% respectively, moisture content decreased from initial value of 89% to 9% in the findings.

Fterich *et al.* (2018) studied mixed-mode forced convection solar dryer and assessed thermal photovoltaic air in the air collector and drying room. The air surrounding the PV panels cooled the PV cells and supplied thermal energy to the drying chamber. The moisture content of the product decreased from 91.94 to 22.32 % for tray 1 and to 28.9 % for tray 2 with a difference of 6.6%. Wang *et al.* (2018) described the Indirect forced convection solar dryer for mango drying testing. The specific rate of moisture extraction was 167 kg/kWh at a drying temperature of 52ºC and the average thermal efficiency ranged from 30.9 to 33.8%. Nimrotham *et al.* (2017) designed a greenhouse solar dryer, the tests for drying takes 52 h to reduce the moisture content from 74% to 13.5% (w.b). The average of air-drying temperature and relative humidity reached to 50ºC and 36%, respectively.

Ismaeel and Yumrutaş (2020) studied the drying system of solar assisted heat pump connected with underground thermal energy storage reservoir and heat recovery unit. The solar drying heat pump constructed by heat pump, heat recovery unit, flat plate, solar collector, drying space and underground thermal energy storage reservoir. Performance analysis model developed to assess the parameters of drying system used heat transfer from thermal energy storage reservoir to utilize heat for drying system components. The experiment tested the performances of heat pump and system, specific moisture evaporation rate, water temperature from thermal energy storage reservoir and energy. The MALTLAB used to obtained results for drying system. Heat pump coefficient, system coefficient, and specific moisture evaporation rate gives 5.55, 5.28 and 9.25 kg $kW^{-1}$ $h^{-1}$, respectively. The tests used mass flow rate of 100 kg $h^{-1}$, cannot efficiency of 40%, area of collector of 100 $m^2$, Reservoir volume of 300 $m^3$.

Bahari *et al.* (2020) researched three types of $Al_2O_3$ nanocomposites to store solar thermal energy for solar dryer and tested the combination of nanoparticles of 0.5, 1 and 1.5% w/w with paraffin wax. The nanocomposites stored in steel pipes as a thermal energy material. The tests results that by adding nanoparticles to paraffin wax, the properties of paraffin wax improved and its energy storage capacity increased. Nanoparticles of $Al_2O_3$ with 0, 0.5, 1 and 1.5% absorbed maximum thermal energy of 3393, 6109, 6445, and 6089 kJ, respectively. Then recommend the use of nanocomposites with 1% of $Al_2O_3$.

Rosli *et al.* (2020) studied a sago pitch waste of original moisture content of 90% (w.b) that can be dried to 10% (w.b) and evaluated the bulk and tapped densities on the moisture content of sago pitch waste used the compressibility index and Hausner ratio to characterize the flow of sago pitch waste in a fluidized bed dryer at wet basis. The temperature between 50 to 80°C and velocity ranged between 1.5 and 2.1 m/s from the supplied air to the fluidized bed dryer as the losses of moisture content, drying rate, and fluidization of drying process. The effective moisture diffusivity analysis showed that the drying process of sago pitch waste dried at air velocity of 1.50 m/s with 80ºC of air temperature and at air temperature of 70ºC with 2.10 m/s of air velocity.

Tuncer *et al.* (2020) described a novel convex - type solar absorber assisted dryer that fabricated for drying municipal sewage sludge. In the experiment unglazed single-pass solar air collector used as main air heater and incorporated to the drying conventional and modified drying space. Experimental method and CFD simulation used to investigate the performance of solar energy assisted dryers. Experimental method obtained average energy efficiency of the modified and conventional indirect solar drying system in the range of 32.85 to 47.09% and 21.32 to 30.45%, respectively.

Poblete and Painemal (2020) investigated the drying process with and without sludge issuing from the coagulation/flocculation of landfill leachate consisted of a rock bed with air preheated by a solar air heater passing through the system.  For thermal storage, the solar energy per mass of sludge was 107.5 kJ/k, measured 240 kJ/kg without thermal storage and 580.5 kJ/kg was measured outside the dryer. The energetic efficiency of the drying process obtained 38.13% and 16.45% for the processes of thermal energy and without thermal storage respectively, the thermal efficiency of 37.8% and 22.2% was obtained during the assessment.

Karthikeyan *et al.* (2021) studied the performance of solar air heater used phase change materials stored in pin fin on absorber surface. Heat loss and outlet air temperature related to thermodynamic efficiency. Paraffin wax as heat energy storage medium selected to improve drying performance when the sun is not active. The thermodynamics improved by 3.1%, and hot air discharge time was hours. César *et al.* (2020) evaluated indirect solar dryer and mixed mode solar dryer. The tomato selected as a sample. During the analysis the maximum temperature inside the drying chamber ranged between 65ºC to 70ºC in mixed mode and 55ºC to 60ºC in indirect solar dryer. The results for tomato dried in indirect solar dryer took 26 h which is longer compared to mixed mode solar dryer which takes 17 h. The solar collector efficiency ranged from 52.3% to 55.45% while the dryer efficiency ranged from 5.47% and 4.48% as reported.

Yadav and Chandramohan (2020) developed a novel numerical model to assess the fins on thermal energy storage device of indirect solar dryer. Simulation was utilized to evaluate two models, one with fins and the other without fins. For both scenarios, use a 4 m/s air velocity. Case 1 and II had average output temperatures of 5.47 K and 9.1 K as reported.

Şevik *et al.* (2019) designed and tested two types of dryers, double pass air solar dryer and infrared assisted double pass solar dryer to ensure continuity of hot air supplied after daytime. Parameters such as mass, heat transfer, coefficient, specific energy consumption, efficiencies and error analysis used to assess thermal and structural performance of solar dryer to test the infrared energy on dried apple slices and mint leaves. The system obtained high collector thermal efficiency of 83.56% for double pass and Infrared assisted double pass solar dryers, energy efficiencies ranged between 1.15% to 8.59% for double pass solar dryer and 2.2% to 26.46% for Infrared assisted double pass solar dryer.

Atalay (2019) studied energy and economic analysis of two energy storage systems for drying purposes. Designed packed bed and phase change material as heat energy storage systems used pebble stones and paraffin wax as heat storage media. A phase change material gives melting temperature of 55 to 60°C. During the charging process, the maximum thermal energy stored was 52.56 MJ and 49.52 MJ, respectively. The test dried a sample of lemon slices with averages of 6.27 hours for pebble stones and 6.23 h for phase change material. The original moisture content of 94.8% lowered to 10% on wet basis. Energy efficiency was found to be 68.2% and 68.55% on average. Economically pebble stone showed low initial investment cost than phase change material.

Alimohammadi *et al.* (2020) described thermal performance of fluid for parabolic trough solar collector. Thermal variations in the receiver tube and storage reservoir were predicted using simulation. The air flow rate of 0.025 kg/s tested for Nano-fluid ($A1_2O_3$, 4%), engine oil (10W40), Glycerin and Water. The study tested to dry apple slices. The results provided thermal energy of 17.36 MJ, 18.46 MJ, 17.76 MJ and 16.8 MJ for Nano-fluid, oil, glycerin and water, respectively.

Lamrani and Draoui (2020) researched the heat performance and economic costs of indirect solar dryer of wood incorporated with thermal energy storage system. The dryer system consisted of drying chamber, solar air collector and packed bed energy storage system. The simulation performed by TRNSYS software predicted the maximum drying relative error of 2.49%. The results revealed that integrating a thermal energy storage system to the dryer permitted it to continue drying the wood while shortening the drying time by 15%. And the payback period of the dryer reduced to 33% equal to 1.85 years.

Pankaew *et al.* (2020) evaluated a large-scale greenhouse solar dryer for drying food products. Because the LPG burner used as a backup heater in the dryer was expensive, a phase change material in the form of a thermal storage medium was designed to replace the LPG burner. The large-scale greenhouse solar dryer integrated with phase change material (latent heat material) used to dry chili. The sample dried from initial moisture content of 74.7% (w.b) to the standard of 10% (w.b) within 2.5 days compared to 11 days of open sun drying. The exergy efficiency for drying chili found to be 13.1%.

Ndukwu *et al.* (2020) researched an active mixed mode wind powered fan solar dryer and a passive mixed mode on wind powered solar dryer tested to dried potato slices. Two dryers tested with and without glycerol as heat energy storage. The ambient temperature ranged from 24 to 50ºC, relative humidity ranged between 10 and 52%. The results showed that active mixed mode wind powered fan solar dryer integrated with glycerol performed drying process for shorter time than a passive mixed mode on wind powered solar dryer. The energy for drying ranged from 4.1 to 4.98 MJ, specific energy ranged from 2.846 to 3.686 kJ/kg, drying efficiency ranged from 25.031 to 31.5%, and exergy efficiency ranged from 14.5 to 80.9%.

Lu *et al.* (2020) described graphite as an added expanded composite phase change material for low temperature heat energy storage and evaluated thermo-physical properties of $KNO_3$ (60.2 wt%)- $LiNO_3$ (29.9 wt%) – Ca $(NO_3)/2$ (9.9 wt%) the results showed the phase transition temperature of ternary nitrate is lower than solar salt but confirmed the great thermal properties.

Kondareddy *et al.* (2020) assessed the performance of the solar tunnel dryer connected with photovoltaic system for dried star fruit. The system consisted tunnel drying chamber, thermal storage unit, paraffin wax as heat storage material, thermal insulator coating material. The test resulted that, the analyses provided the higher values of 47.59 g of sample and 73.59 μ mol gram of sample. Azaizia *et al.* (2020) researched a mixed mode solar greenhouse drying system with and without heat energy storage unit. Paraffin wax used as phase change material for drying red pepper. The results showed that using phase change material during the night time resulted in a maximum drying temperature of 75ºC and a relative humidity of 18.6%. The moisture content has an effective reduction of 95% in 30 h for dryer with phase change material, in dryer without phase change material took 55 h and in open sun drying took 75 h.

Gabisa and Aman (2016) researched solar thermal energy storage for cooking application. The 1.4 kg PCM charged up to 300ºC for 50 minutes, while discharged from 300ºC to 100ºC for 4.5 h. Discussed $NaNO_3$ (60%): $KNO_3$ (40%) were the appropriate choice for potential cooking by storing the cheapest solar thermal energy and good thermal characteristics.

Several researches addressed the poor performance of passive solar dyers compared to those combined with the heat storage system. Thus, further studies are needed to design solar dryers, which are incorporated with heat storage systems to preserve more heat that can be used in absence of active sunlight. The combination of potassium nitrate ($KNO_3$ (40%)) and Sodium nitrate ($NaNO_3$ (60%)) known as a nitrate salt is a good example of heat storage material that has excellent thermal properties as assessed by Gabisa and Aman (2016). The solar dryers have not yet utilized these nitrates as a heat storage medium. Most of the studies have used it for power generation and cooking applications. Carefully, this study found its performance as a heat storage medium used in a solar dryer integrated with heat storage system. The solar dryer was constructed and integrated with a low-cost solar dish concentrator to maximize the collection of solar energy and store it in the thermal storage materials used when sunlight is not present.

# CHAPTER THREE

# MATERIALS AND METHODS

## 3.1 Materials

The self-acting temperature control (Spirax sarco SA 121) for controlling temperature purchased at a pressure and vessel equipment store in Arusha (Fig. 9). Two packages of potassium nitrate (40%) and three packages of sodium nitrate (60%) each carried out 500 g were purchased from the local market in Arusha, this mixture has been used by many other researchers in solar cookers but has not been used in solar dryers. Tanzania and used as a heat storage medium. Other materials such as flat glass mirror (ASTM C 1503), clear transparent glass (4 mm), steel square channel (30 mm$^2$), stainless steel sheet (2 mm) and aluminum sheet (2 mm) were sourced locally in Arusha, Tanzania for fabricated solar dryer. The 3000 g of fresh red peppers were selected from the local market, Arusha, Tanzania for the purpose of drying tests (Fig. 21).

## 3.2 Study Location

This study was carried out in the Nelson Mandela African Institution of Science and Technology (NM-AIST) at Tengeru Campus that located 16 km east of Arusha City Centre, Tanzania in 3.3995º S, 36.7968º E geographical coordinate. The solar dryer, integrated with heat energy storage system was designed, built and tested under Tanzania's climatic conditions.

## 3.3 Design Considerations

### 3.3.1 Temperature

The standard temperature for drying food products ranges from 30 to 65ºC. Therefore, 45ºC and above is considered average and normal for drying vegetables, fruits, roots, seeds, herbs, rice, grains, fish and meat (Alamu *et al.*, 2010).

### 3.3.2 Efficiency

Efficiency is the ratio of the useful work performed by a dryer process to the total energy expended or heat taken in.

### 3.3.3 Air Vents

The air vents provide air circulation which is suggested for a solar dryer, so 7 mm drilled holes were created around the bottom and top sides (Fig. 7).

### 3.3.4 Solar Collector (Glass)

It is suggested that the transparent glass cover should have a thickness of 4 to 5 mm, where the glass used as solar collector was 4 mm and (80 x 84) $cm^2$ (Bakari *et al.*, 2014).

### 3.3.5 Dimension

The average dimensions of the drying chamber were made around (80 x 80 x 40) $cm^3$ with an inclination angle of 13º and air vent at bottom and top side. The drying chamber was covered with transparent glass (80 x 84) $cm^2$ at the top side (Fig. 7).

### 3.3.6 Trays

Two grilled trays were made of stainless-steel bars covering approximately (75 x 75) $cm^2$.

### 3.3.7 Solar Dish

The solar dish collector has an aperture diameter, depth of the dish and focal point where the direct radiation concentrates after reaching the reflective surface.

### 3.3.8 Reflective Material

The mirror with reflective surface was used because of the recommendable average value of reflectivity in the solar spectral range of between 0.7 and 0.95.

### 3.3.9 Cavity Receiver

Receives/absorbs the reflected solar radiation from the dish collector which is converted into heat energy for drying purposes.

## 3.4 Design and Construction Procedure

The construction took place in three stages, starting with the drying chamber, solar dish collector and cavity receiver. Then the three components were assembled and positioned in the area of study along the N-S axis to track the sun for data collection and experimentation along the equatorial latitude. The manual trucking mechanism was designed to direct the solar dish to face the sun's ray’s perpendicular to the parabolic dish concentrator and to allow the reflection to the focal point that stays in line with one axis. The solar dryer was directly exposed to the solar radiation intensity to provide heat accumulation at focal point under the cavity receiver which secured the heat in the thermal storage media. The rotation of the solar dish concentrator and sun tracking mechanism are shown in Fig. 4.

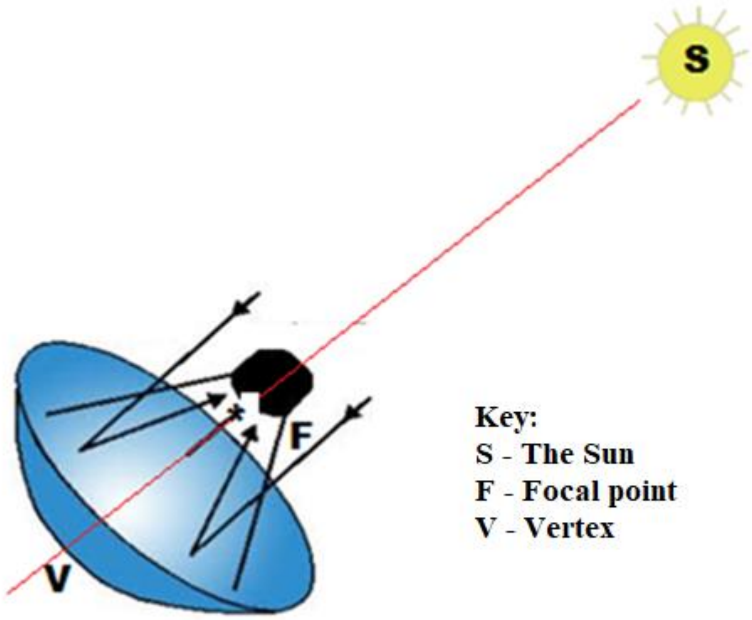


**Figure 4: Orientation of parabolic solar dish concentrator and sun tracking system (Joardder *et al.*, 2017)**

### 3.5 Solar Collector Design

The inclination angle of solar collector (β) from the horizontal surface was found by using the following formula as calculated by Ugwuoke *et al.* (2019).

$$\beta = 10^{\circ} + Latitude\theta \tag{1}$$

Where:

Latitude θ = 3.3995ºS (Latitude of the study at Arusha)

Therefore, the collector inclination angle = 10° + 3.3995ºS = 13.3995º.

### 3.5.1 Solar Thermal Collector Efficiency

The collector thermal efficiency and drying efficiency of the solar dryer was expressed by using the following formula (Mehta *et al.*, 2018):

$$\text{Collector Efficiency, } \eta_c = \frac{v\rho\Delta T C_p}{I_c A_c} \times 100\% \tag{2}$$

Where:

V is the volumetric flow rate of air in $m^3/s$, P is the air density in $kg/m^3$, $\Delta T$ is the air temperature elevation in °C, $C_p$ is the air specific capacity in J/kgK, $I_c$ is the insolation at the collector surface in $W/m^2$ and $A_c$ is the collector area in $m^2$.

## 3.6 Parabolic Collector System

In the present study, the working principles of the parabolic collector system were examined and the vital areas of interest concerned parabolas and parabolic collectors were highlighted. The solar dish refers to the characteristic of reflecting any incident solar radiation parallel to its focal point axis. This is the general principle that is used in most parabolic solar concentrator dish and parabolic trough collectors where large amounts of concentrated heat are generated in the focus and then converted into useful heat energy. The parabolic equation refers a point locus that moves the same distance from a fixed line and a fixed point is called a parabola. The fixed line is called a directory and the fixed point is the focus (F). The perpendicular line to the directory that passed through the focus (F) is called the parabola axis. The vertex intersects the parabolic dish trough point (V) which is exactly the centre or midway (Mohamed *et al.*, 2012). The parabolic geometry is shown in Fig. 5.

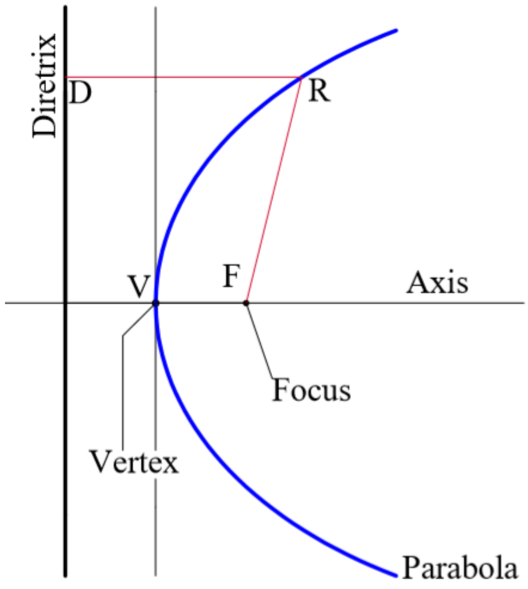


**Figure 5: Parabolic geometry**

### 3.6.1 Geometric Concentration Ratio

The ratio of concentration relates directly to reflector quality. The concentration ratio of the geometric ($CR_g$) is written as the ratio of aperture area of a parabolic dish ($A_a$) to the receiver base area ($A_r$), and it is found as:

$$CR_g = \frac{A_a}{A_r} \tag{3}$$

### 3.6.2 Angle of Reflection

By Suell's law the incidence angle is equal to the angle of reflection. All solar radiation that comes parallel to the parabola's axis reflected back to a focal point called the focus. The P is the distance RF. So, reflection angle (Ψ) is given as:

$$\psi = 2p \tag{4}$$

### 3.6.3 Rim Angle

Rim angle is the ratio between the lengths of the focal (f) to the dish diameter or the width of the aperture (d). For typical parabola, the depth of the curve (h) is sometimes measured from top to bottom of the curve called the height or depth of the parabola. The focal length is measured from the focus (F) to the vertex (V). The rim angle ($\Psi_{rim}$) it can be calculated by the following Equation:

$$\tan \psi_{rim} = \frac{1}{\left(\frac{d}{8h}\right) - \left(\frac{2h}{d}\right)} \tag{5}$$

Therefore, rim angle $\Psi_{rim} = 63.9°$.

Arc length (s) of the parabola is another important property of the parabola used when designing the solar concentrator and is calculated by the following formula:

$$S = \left[\frac{d}{2}\sqrt{\left(\frac{4h}{d}\right)^2 + 1}\right] + 2f \ln\left[\frac{4h}{d}\sqrt{\left(\frac{4h}{d}\right)^2 + 1}\right] \tag{6}$$

The parabolic dish surface area can be given using the following Equation:

$$A_{sc} = \frac{8\pi f^2}{3}\left[\left(\left[\frac{d}{4f}\right]^2 + 1\right)^{\frac{3}{2}} - 1\right] \tag{7}$$

Where:

$A_{sc}$ is the parabolic dish surface area in $m^2$, f is the focal point in m and d is the aperture diameter in m.

### 3.6.4 Segment of a Parabola

The size of the curve was specified in terms of a linear dimension by looked the focus point (f), rim angle ($\Psi_{rim}$) and aperture diameter (d). The segment of a parabola shared a focal point with the same aperture width gives a different rim angle with respect to parabola height as shown in Fig. 7.

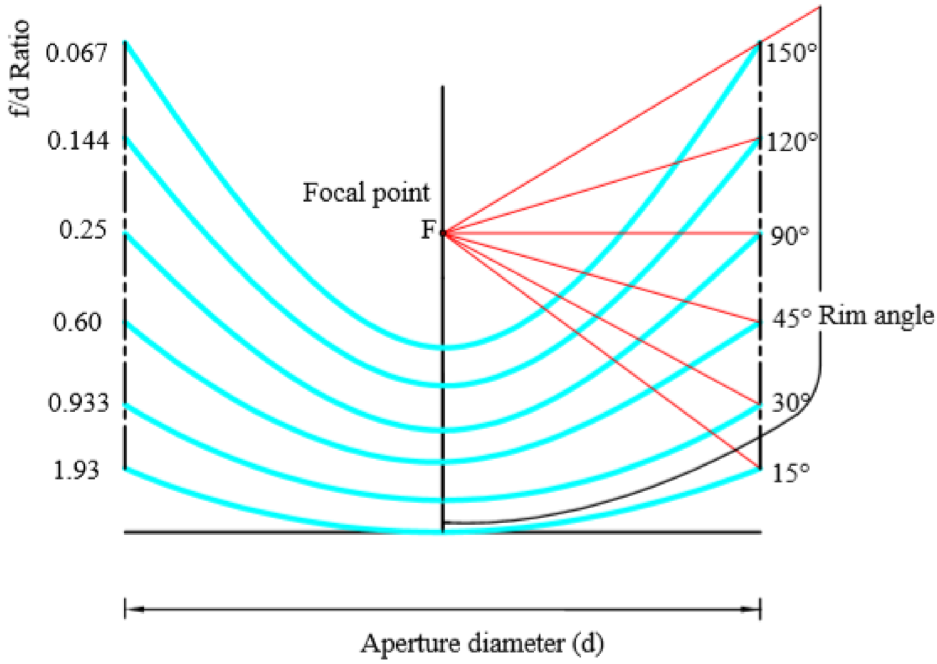


**Figure 6: Segment of a parabola having a common focus point and rim angle with the same aperture diameter**

### 3.6.5 Design Parameter and Dimensions of the Solar Parabolic Dish Concentrator

Table 2 summarizes all important design parameters of the parabolic solar dish concentrator such as aperture diameter, focal length, concentrator depth, vertex, rim angle.

**Table 2: Design dimensions of the parabolic solar dish concentrator**

| S/No. | Parameters | Numerical value | Unit |
|---|---|---|---|
| 1 | Aperture diameter ($d_a$) | 1 | M |
| 2 | Focal length (f) | 0.4 | M |
| 3 | Depth of the concentrator (h) | 0.15625 | M |
| 4 | Vertex (V) = d / 2 | 0.5 | M |
| 5 | Rim angle ($\Psi_{rim}$) | 63.9 | o |
| 6 | f/d | 0.4 | - |

## 3.7 Cavity Receiver

The cavity receiver is the component used to collect the maximum amount of solar radiation that was reflected back to the focal point with the parabolic dish concentrator acting as a heat source. The cavity receiver was made of 2 mm thick stainless-steel plate and cylindrical pipe, covered with a thin layer of gray paint and placed at a focal point of the parabolic solar dish. The receiver-aperture area is found using the equation (8):

$$A_r = \frac{\pi}{4} d_r^{\ 2} \tag{8}$$

Where:

$A_r$ is the receiver aperture area in m and $d_r$ is the receiver diameter in m.

Therefore, $A_r = 0.008107\ m^2$

### 3.8 Drying Chamber

The drying chamber consists of sheets of aluminum and structures of steel and covered with a glass plate solar collector lilted at 3.9º. The base area is approximately (80 cm x 80 cm), a small hole was drilled at the bottom around the base and near the solar collector to allow air circulation and painted black inside to absorb more solar radiation. Inside the drying chamber, two trays are fitted to support the dried products. Aluminum material was selected to construct the drying chamber due to the properties as shown in Fig. 7.

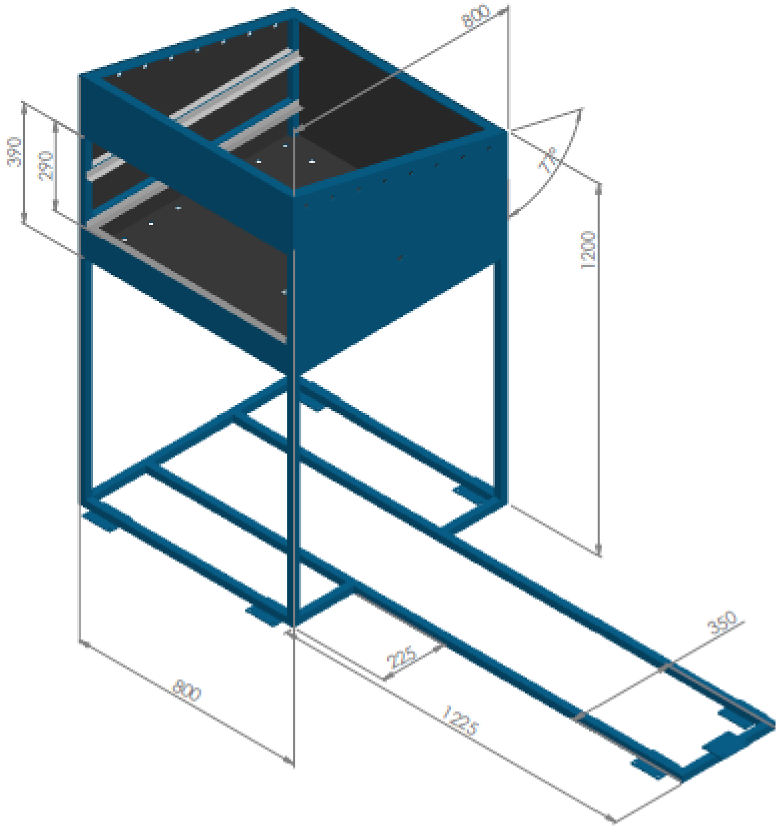


**Figure 7: Drying chamber**

### 3.9 Solar Dryer Testing

Naturally ventilated effectively performed when the surrounding air moves away from the product after absorbing moisture and replacing it with less humid. In the design stage, this factor was considered. The hot air is recirculated by natural convection due to the pressure difference, so that the temperature inside the drying chamber is constant to prevent the formation of vacuum inside the solar dryer so that the small holes of 7 mm diameter were provided around the base of the drying chamber and at the top near the solar collector.

#### 3.9.1 Instrumentation and Measurement

The SNN – USB temperature/humidity data loggers with the accuracy of ±0.3°C, ±3% and measurement range of -40 to 125°C, 0 to 100% RH respectively, were used to measure the relative humidity and temperature in different locations, ambient temperature ($T_a$), drying chamber ($T_d$) and heat storage media ($T_m$) and the measurement range were -40 to 125°C, 0 to 100% RH. The readings were recorded after every two minutes starting from 9:00 to 21:00 h.

Anemometer (Kestrel 1000 wind meter) with the accuracy of the measurement 0.6 to 60.0 m/s or 1.3 to 89.5 mph was used to measure the wind speed and the solar power meter (TES - 132 Data logging) with measuring range of 2000 W/m² and accuracy within ±10 W/m² or ± 5% was used to measure and to record the solar radiation with the connection of the laptop.

### 3.9.2 Experimentation

The experiment was conducted to assess the performance of the solar dryer, integrated with the heat energy storage system. The measured data included ambient, drying, medium temperature heat storage, relative humidity, and solar radiation. During the performance evaluation the weather conditions were cloudy and sunny. The initial moisture content of red peppers was found by using the oven drying method. The sample was weighed using USS – DBS2 digital analytical balance scale of measurement range 0 - 5000 g and accuracy of ±0.01 g. One kg of hot red peppers was placed in hot oven at 60ºC for 12 h, the initial moisture content was found to be 86%. The moisture content was computed from the experimental data.

### 3.9.3 Experimental Setup

The primary specific objective of the study was to develop solar dryer, integrated with heat energy storage system, so the basic idea came from passive solar dryers through integrated heat storage system and decided to use parabolic concentration system. The experimental setup consisted of solar parabolic dish collector, cavity receiver, temperature control system, glazing, drying chamber and main frame. Nitrate salt was used as a medium for heat storage and filled in the cavity receiver's inner cylinder as shown in Fig. 8.

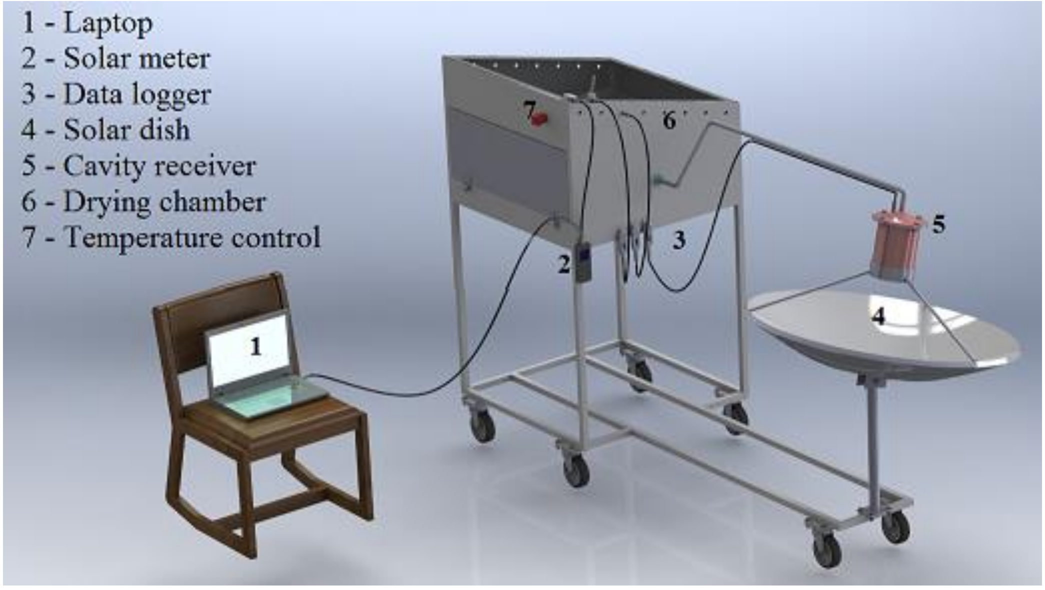


**Figure 8: Experimental setup**

### 3.10 The Self-acting Temperature Control

The knob was connected to a temperature sensor inside the drying chamber; the desired temperature can therefore be set. As the temperature goes above the set temperature, the valve is automatically closed by the actuator, and if the temperature goes below the set temperature, the valve is automatically opened by the actuator. The temperature control valve consists of a sensor, capillary tube and actuator; these components are connected to the 2-port control valve. If a sensitive fluid is heated, expand faster and contract if it is cooled. The force created by the expansion or contraction is transferred to the actuator through the capillary to open or close, to allow or stop the flow of hot air through the control valve. The adjustment knob is turned clockwise to decrease the set temperature, and vice versa to raise the set temperature as shown in Fig. 9.

#### 3.10.1 Specification of Temperature Control System

Type: SA121 (Spirax sarco)

Range: 1

Temperature: -15 to 50 ºC

Maximum sensor temperature: 55ºC over set value to max 190ºC

Material: Brass

Weight: 2.0 kg

Standard length of capillary tube: 2 m

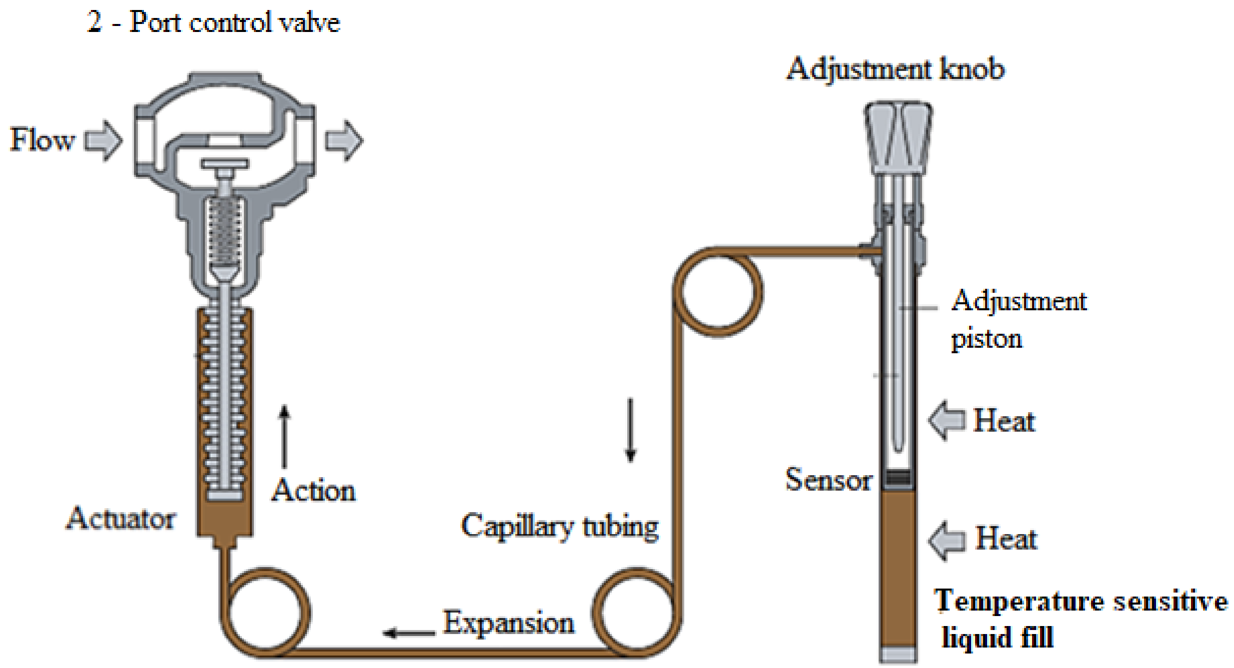


**Figure 9: Self-acting temperature control system (Spirax sarco SA121)**

### 3.11 Heat Energy Storage Medium

The nitrate salt (60% Sodium nitrate, 40% Potassium) as heat storage media was selected due to its thermal properties, suitable heating rate and its operating temperature and was taken into account for many factors, such as storage duration, the temperature required, storage capacity, heat losses, economy and space availability. The use of heat energy from the nitrate salt required heat charging, heat storage and heat discharge as shown in Fig. 10.

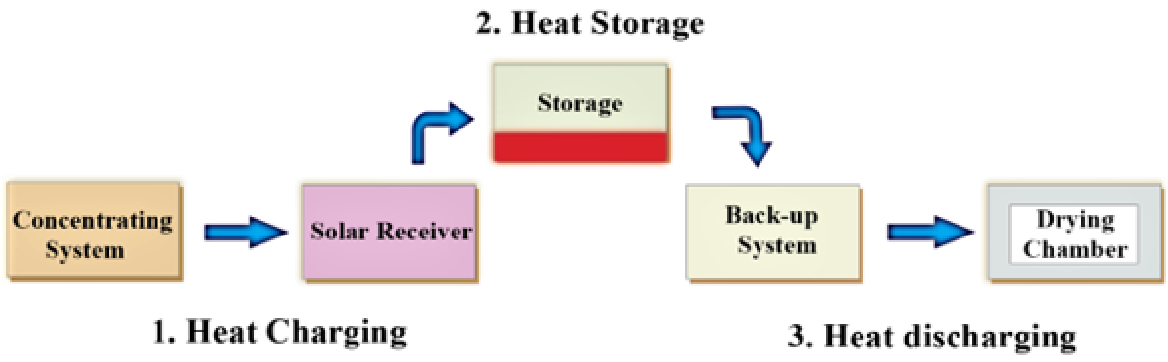


**Figure 10: Utilization of heat energy**

## 3.12 Solar Dryer Performance Analyses

### 3.12.1 Error Analysis

An error occurs due to difference between the actual value and the value indicated by the measuring instruments. During experimental analysis temperature measurement, relative humidity, moisture loss, weight loss, solar intensity and air velocity, errors were undertaken via solar dryers integrated with heat energy storage system. In order to determine the total error in the measuring instruments fixed, manufacture and random errors were considered (Gulcimen *et al.*, 2016). If x represents the amount of error in each variable of the measurement, the total error can be found by:

$$W_{th} = [(x_1)^2 + (x_2)^2 + \cdots (x_\infty)^2]^{1/2} \tag{9}$$

Table 3, shows the total errors in measurement that found in solar dryer integrated with heat energy storage system. These errors are caused by the measuring instruments such as data loggers, solar power meter, anemometer and digital balance scale.

**Table 3: Total errors made in drying experiments**

| Instrument used | Parameter(s) causing error(s) | Unit | Total error |
|---|---|---|---|
| Data Logger | Total error from heat (Temperature) | | |
| | $W_{Ta}$ – Ambient temperature | ºC | ± 0.3 |
| | $W_{Tc}$ – Drying temperature | ºC | ± 0.3 |
| | $W_{Th}$ – Heat storage material temperature | ºC | ± 0.3 |
| Data Logger | Total error from relative humidity | | |
| | $W_{Hr}$ – Relative humidity | % | ± 3 |
| Digital balance scale | $W_M$ - Weight | G | ± 0.01 |
| Solar power meter | $W_S$ - Solar radiation intensity | W/m$^2$ | ±10 |
| Anemometer | $W_V$ – Air velocity | m/s | ± 0.104 |

### 3.12.2 Efficiency Analysis

A solar dryer integrated with heat energy storage system was used for the drying test in the experiment conducted. The following function expresses the change in air temperature (ΔT).

$$(\Delta T) = f(I_c, A_c, \tau\ \alpha, E_i) \tag{10}$$

Thermal efficiency of a solar collector is the ratio of useful heat gain over any time period to the incident solar radiation over same period, can be calculated by using the following Equation:

$$\eta_c = \frac{m\ c_{p\ \Delta T}}{I_c\ A_c} \tag{11}$$

## 3.13 Drying Characteristics Analyses

### 3.13.1 Moisture Content

The amount of water found in a wet sample can be defined as the moisture content. The moisture of the product depends on the condition of the surroundings like relative humidity or temperature and it can be expressed in wet or dry basis. The amount of moisture to be removed from red peppers analyzed (Bhardwaj *et al.*, 2019):

$$MC_{wb} = \left[ \frac{(M_t - M_f)}{M_t} \right] \times 100\% \qquad (12)$$

Where:

$MC_{wb}$ is the moisture content for dry basis in %, $M_t$ is the initial mass of sample in kg and $M_f$ is the final mass of sample in kg.

### 3.13.2 Drying Rate

The drying rate is the amount of evaporated moisture per unit time and analyzes the system effectiveness that takes place during the drying period. Mathematically, it is calculated as:

$$DR = \frac{dM}{dt} = -k(M_t - M_e) \qquad (13)$$

$$\frac{dM}{(M_t - M_e)} = -kdt \qquad (14)$$

Where:

DR is the drying rate; $M_t$ is the moisture content at any time t and $M_e$ is the equilibrium moisture content.

### 3.13.3 Moisture Ratio

The moisture ratio was determined using the following Equations:

$$MR = \frac{(M_t - M_e)}{(M_i - M_e)} \qquad (15)$$

$$MR = \frac{M_t}{M_i} \qquad (16)$$

Where:

MR is the drying rate, $M_t$ is the moisture content at any time t, $M_e$ is the equilibrium moisture content and $M_i$ is the initial moisture content.

### 3.13.4 Amount of Moisture Removed

Moisture content on wet basis is the amount of water per unit mass of moist or wet sample.

The formula used to determine the total amount of moisture of wet sample, $M_w$ is expressed as:

$$M_w = \frac{(M_i - M_f)}{M_i} \, x \, 100\% \quad (17)$$

$$M_w = \left(\frac{1000-140}{1000}\right) \times 100\% = 86\% \quad (18)$$

Where:

$M_i$ is the initial mass of sample = 1000 g.

$M_f$ is the final mass of sample = 140 g.

$M_w$ is the amount of moisture on fresh red peppers = 86%

# CHAPTER FOUR

# RESULTS AND DISCUSSION

## 4.1 Overview

The performance evaluation of Solar Dryer, integrated with the heat energy storage system, was carried out in October 2018 at the Nelson Mandela African Institution of Science and Technology. The tests took place for a week every day for 12 h from 9:00 to 21:00 hours. After designed the solar dryer, integrated with heat energy storage system to be completed various tests were conducted to evaluate the performance of the solar dryer integrated with heat energy storage system. Red peppers were selected as a sample to be dried during the drying test. The results of the various tests were recorded and analyzed as discussed in this chapter. The designed solar dryer is shown in Fig. 11.

**Figure 11: Designed solar dryer integrated with heat energy storage system**

## 4.2 Dryer Evaluation Tests

After completing the construction of the dryer, different tests were performed in order to evaluate its performance the solar dryer integrated with heat energy storage system and found to be more efficient on drying the red pepper as compared to open sun drying system. In two days of continuous drying under the same climatic condition used the solar dryer, a total of 76% of moisture content was removed from sample and remain the required 10% compared to three days of open sun drying. The assessment of the solar dryer, integrated with or without heat energy storage system was done using two different tests. The findings showed the temperature of the heat storage medium was much higher than the ambient and air-drying temperature at most daylight hours. Each test is discussed below.

The experiments were done without loading and load drying tests started at 9:00 h and stopped at 21:00 h every day for six days. The drying rate was determined by loading the dryer with red peppers. The important parameters affecting performance of the dryers were measured and recorded accordingly. The experimental setup made up with solar dish collector, cavity receiver, temperature control system, glazing, drying chamber and main frame were used. Nitrate salt was used as a thermal storage material. The following analysis was performed and recorded to investigate the efficiency of the solar dryer, integrated with heat energy storage system. The variation in ambient air temperature with time was ranged from 19.3 to 37.4°C within six days of experiments as shown in Fig. 12.

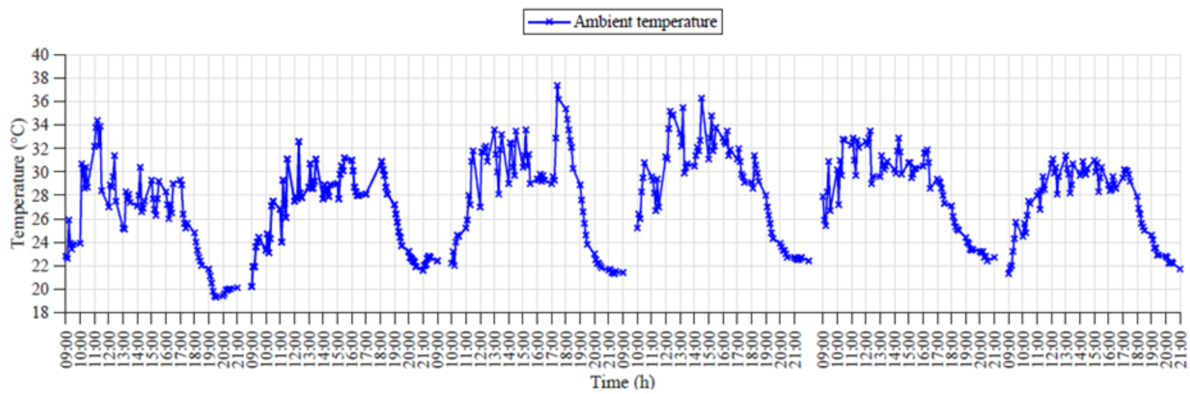


**Figure 12: Variations of ambient temperatures with time (day 1- 6)**

During the days of experiments the change of relative humidity of the atmospheric air was found between 28.3% and 77.8% as shown in Fig. 13.

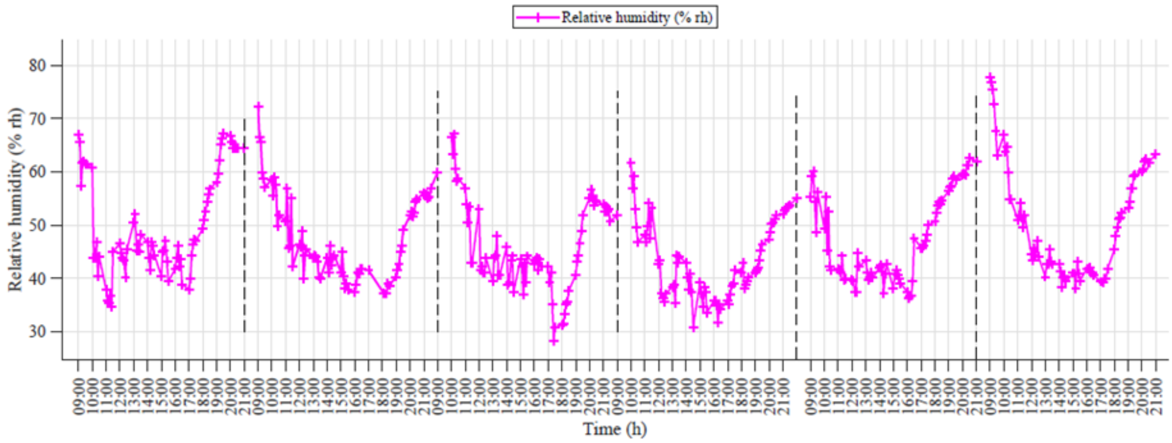


**Figure 13: Variation of relative humidity with time (day 1 - 6)**

The findings showed that, temperature rises and falls with increasing and decreasing of solar radiation intensity that varies at a day and goes down in the evening. The average solar radiation was 610.4 W/m² where the solar intensity ranged from 1.5 to 1327 W/m² recorded from 9:00 to 18:00 h for 6 days of experimental. The parabolic solar dish collector was oriented manually to track the movement of the sun in intervals of every 15 minutes to ensure efficient of solar dish as shown in Fig. 14.

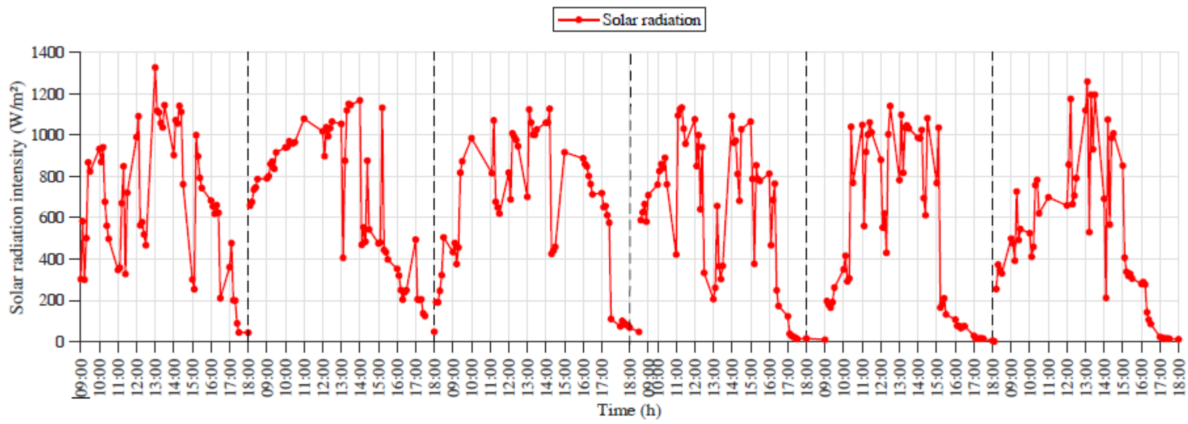


**Figure 14: Variation of solar radiation intensity with time during experimental days**

Without a load test was performed to assess the solar dryer without the application of a heat storage system, during the experiments the temperature control valve was closed every day from 9:00 to 17:00 h for four days. The average ambient air temperature was 27.7°C, while the maximum of air-drying temperature, heat storage medium and solar intensity was 62.4°C, 125°C and 1327 W/m², respectively. The temperature control valve was opened in the evening at 17:00 h under no load condition to allow the application of a heat storage system, the average reading of air-drying temperature, heat storage medium and solar intensity was found to be 46°C, 81.7°C and 628.9 W/m² then dropped to 19.6°C, 18.3°C and 1.5 W/m², respectively as shown in Fig. 15.

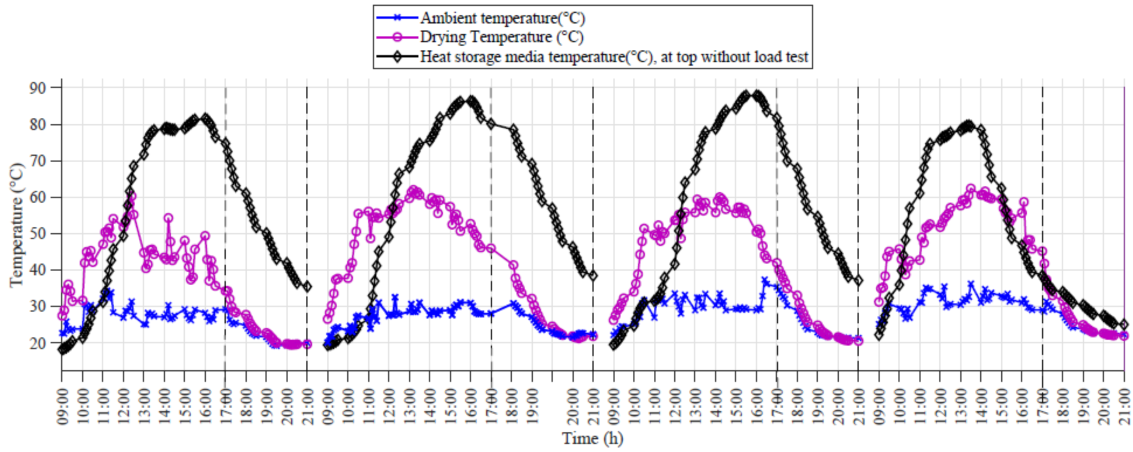


**Figure 15: Temperature variation with time without load tests (day 1 - 4)**

The top and bottom side maximum heat storage media temperature for without load tests were ranged between 87.8°C and 125°C, respectively. The weather was cloudy and sunny during the tests as shown in Fig. 16.

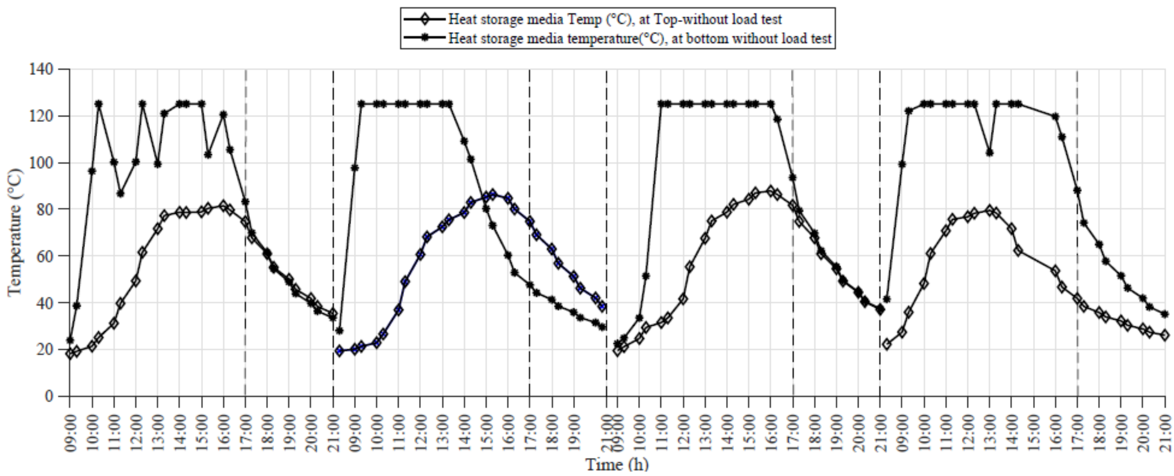


**Figure 16: Heat storage temperature variation with time (without load tests) day 1 - 4**

During the load drying tests the temperature control valve was closed at day time and opened when sunrise missed for assessment, the experiments were conducted between 9:00 h and 21:00

h for two days. The ambient ranged from 21.3 to 33.5°C, drying air ranged from 33.6 to 60.9°C, heat storage medium temperature ranged from 20.6 to 125°C and solar radiation intensity ranged from 44 to 1327 W/m², then temperature proceed to decreased slowly at the evening while the heat storage system continuous to utilize thermal energy as shown in Fig. 17.

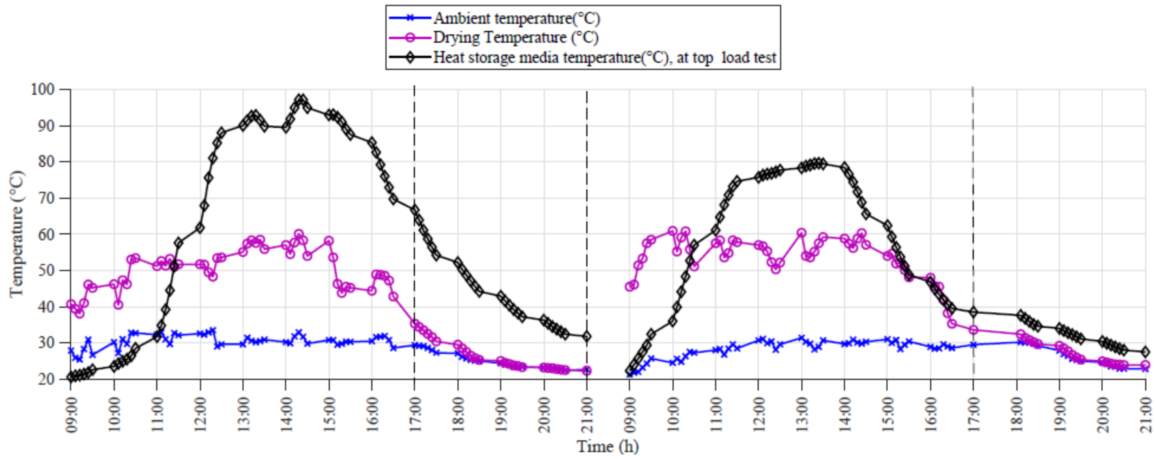


**Figure 17: Temperature variation with time (Drying tests) day 5 - 6**

During the drying tests, the maximum temperature of heat storage material at top and bottom side were 81.7°C and 125°C respectively as shown in Fig. 18.

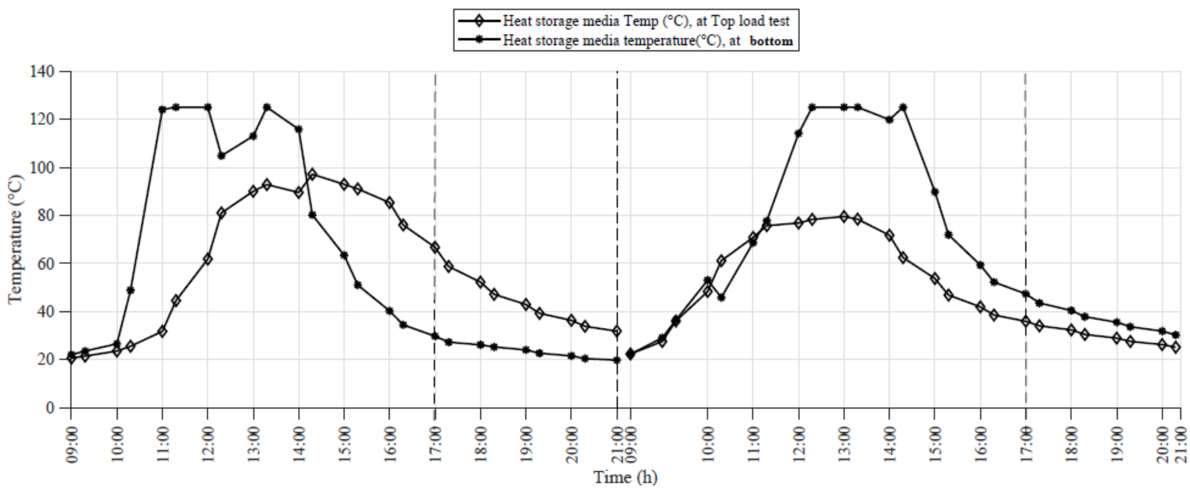


**Figure 18: Heat storage medium temperature variation with time (Drying time) day 5 - 6**

For comparison studies between the solar dryer and sun drying, 2 kg of fresh red peppers were selected to be dried. The fresh red peppers were assessed and provided an original moisture content of 86% (w.b), 1000 g of sample was dried in solar dryer and reduced to a desired moisture content of 10% (w.b) for 24 h. Likewise, open sun drying took 36 h to decrease the moisture content from 1000 g to achieve 10% (w.b) as shown in Fig. 19.

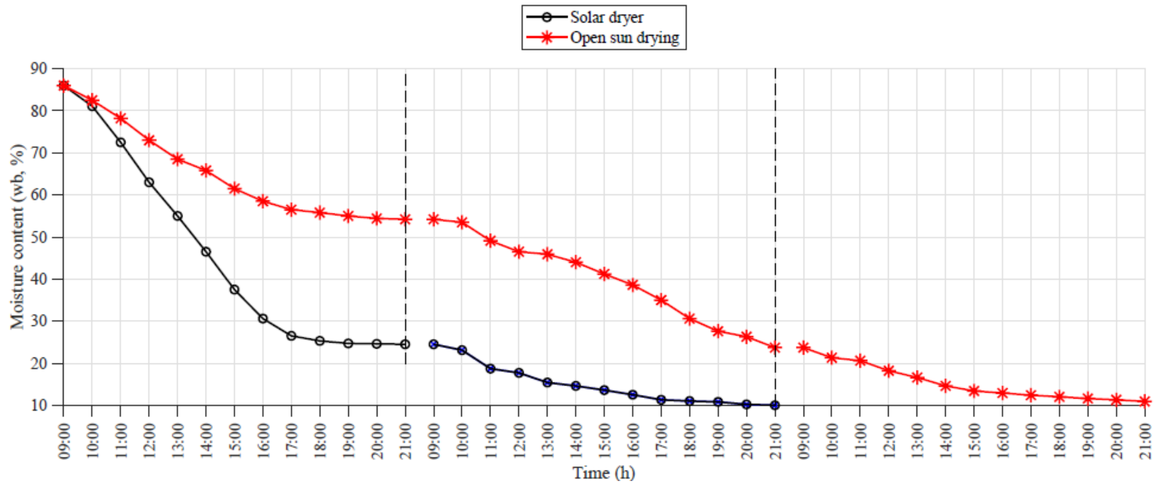


**Figure 19: Moisture content loss (w.b) with time for solar dryer and open sun drying**

The weight and moisture content loss of drying red peppers was evaluated to check the overall drying performance of solar dryers integrated with heat energy storage system as shown in Fig. 20.

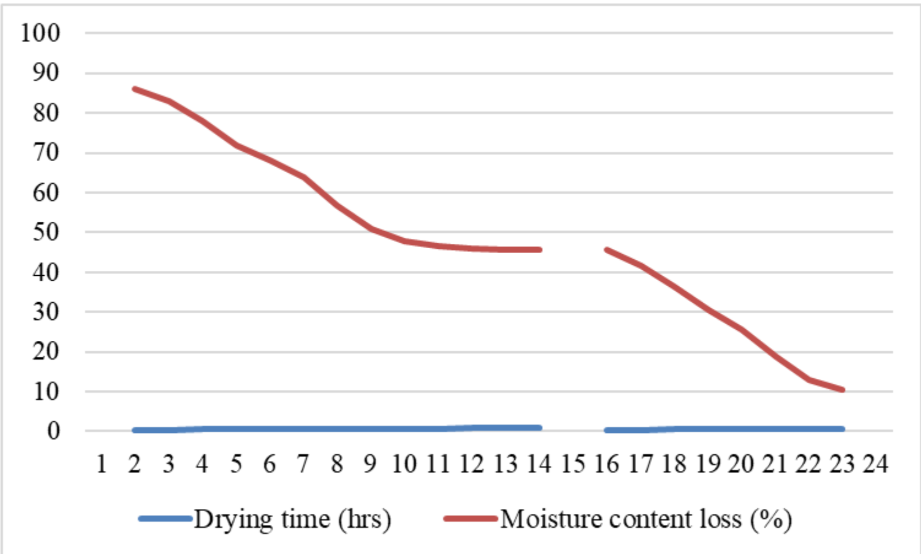


**Figure 20: Moisture content loss and drying time**

The findings showed that the dried one in the solar dryer was better preserved without losing nutrients colour, and flavour compared to the ones dried in the open sun that appeared to be pale, lose their good appearance and it was also infested with dust and insects as shown in Fig. 21.


**Figure 21: (a) Fresh red peppers before drying, (b) Red peppers after solar drying, (c) Red peppers after open sun drying (Missana, 2020)**

During the assessment the average variations of the wind speed during the days of drying test. Air velocity for the location of study was recorded from 9:00 to 16:00 h in interval of every 10-minute to show an air velocity at the area of study. The average wind speed for 6 days was 1.7 m/s as shown in Fig. 22.

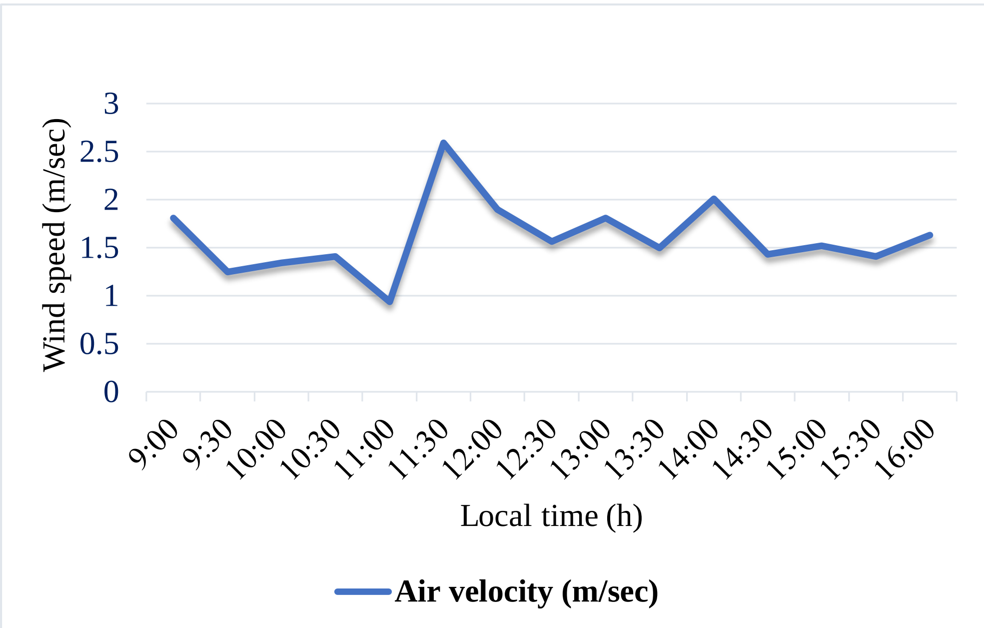


**Figure 22: Air velocity**

### 4.3 Analysis of the Drying System Performance

The performance of the solar dryer, integrated with the heat energy storage system assessed. Ambient, drying air, medium temperature, relative humidity, and solar radiation was measured. The oven drying and experimental methods were used respectively. The USS – DBS2 digital analytical balance scale was used to measure the sample weight, the readings were recorded and taken from 9:00 to 21:00 h. Anemometer was used to measure the wind speed, solar power meter was used to measure the solar radiation with connection of the laptop and the USB data loggers with the accuracy of ±0.3°C, ±3%, were used to assess the relative humidity, ambient, drying chamber and heat storage media temperatures. The initial moisture content was found from the experimental data by placed 1000 g of red peppers in hot oven sets at 60ºC for 12 h that decrease to 140 g which dried to required standard. The initial moisture content of fresh red peppers was 86% as Equation 34 expressed. The design data and detail of the solar dryer integrated with heat energy storage system which has been used in this study is illustrated in Table 4.

**Table 4: The design data and detail of solar dryer**

| S/No. | Description | Detail |
|---|---|---|
| 1 | Air drying temperature | 19.6 – 62.4°C |
| 2 | Cover plate material (solar collector) | Clear glass (4 mm) |
| 3 | Solar collector area | 0.8 m x 0.84 m |
| 4 | Drying area | 0.8 m x 0.8 m |
| 5 | Type of solar dryer | Active mixed mode |
| 6 | Number of trays | 2 |
| 7 | Size of tray | 0.75 m x 0.75 m |
| 8 | Material of tray | Stainless steel |
| 9 | Material for drying chamber | Aluminium sheet 1.5 mm |
| 10 | Reflective material | Mirror (reflectivity 0.95) |
| 11 | Collector tilt angle | 13.9º |

### 4.4 Collector Efficiency

Collector efficiency measures the thermal performance and the useful heat energy gain of the collector. Not all of the solar radiation from the sun incident on the collector surface is converted to heat although its inclination angle was 13.3995º. Part of the radiation is reflected back to the sky and the other component is absorbed by the glazing. Once the collector absorbs heat and as a result temperature gets higher than the ambient temperature, there will also be a heat loss to the atmosphere by convection and radiation. Collector efficiency of the solar dryers was determined by using the Equation 2 in Chapter 3.

## 4.5 Economic Analysis of the Solar Dryer, Integrated with Heat Energy Storage System

Due to the inefficiency of drying food products and crops using passive solar dryers, the drying time, efficiency and quality of food products can be improved by integrating the passive solar dryer with other systems that can store energy for later use. The selection of the economic heat storage system is therefore the main challenge involved in implementing the optimum system under different climatic conditions. For developed solar dryer system, this study proposed a cost effective and affordable heat storage system. The economic analysis was conducted on the basis of the developed system's cost and payback period.

### 4.5.1 Economic Parameters and Cost

Economic parameters and costs were found to be:

(i) Rate of inflation 3%.

(ii) Rate of interest 9%.

(iii) Life span of the solar dryer is 22 years.

(iv) The cost of fresh red pepper were Tanzanian Shillings (TZS) 2500 per kilogram.

(v) The price of drying red pepper will be Tanzanian Shillings 1000 per kilogram.

(vi) Savings will be Tanzanian Shillings 1000 per day for 1 year (Tanzanian Shillings 365 000).

### 4.5.2 Solar Dryer Costs

Capital costs ($C_c$) of a solar dryer, integrated with heat energy storage system are the sum of all the components and fabrication costs. Production cost ($P_c$) comprises the sum of capital costs ($C_c$), costs of fresh materials ($F_{mc}$), labour charges ($L_c$) and maintenance costs ($M_c$). The production costs can be written as per Fudholi *et al.* (2015).

$$P_c = C_c + F_{mc} + L_c \tag{19}$$

Where:

Capital cost ($C_c$) = TZS 1 800 000

Costs of fresh materials ($F_{mc}$) = TZS 50 000

Labour charges ($L_c$) = TZS 150 000

Therefore, production costs ($P_c$) = TZS 2 000 000

The estimated costs and materials components used to make the solar dryer integrated with heat energy storage system are shown in Table 5.

**Table 5: Cost estimated for solar dryer components, integrated with heat energy storage system**

| S/No. | Components/Parts | Quantity | Cost (TZS) |
|---|---|---|---|
| 1. | Drying chamber and Main frame | 1 | 350 000 |
| 2. | Trays (stainless steel) | 2 | 250 000 |
| 3. | Solar collector (Glazing) | 1 | 50 000 |
| 4. | Solar dish collector | 1 | 250 000 |
| 5. | Sun tracking mechanism | 1 | 50 000 |
| 6. | Temperature control system | 1 | 450 000 |
| 7. | Fabrication | - | 200 000 |
| 8. | Nitrate salt | - | 200 000 |
| **Total capital cost ($C_c$)** | | | **1 800 000** |

The profit ($P_r$) will be realized after the solar dryer starts working and can be defined as the difference between total sales ($T_s$) with all types of spending such as production costs and can be written as:

$$P_r = T_s - P_c \tag{20}$$

Return of capital ($R_c$) is influenced by time after the solar dryer starts working and it can be written as:

$$R_c = \frac{P_r}{C_c} \tag{21}$$

### 4.5.3 Payback Period

Payback ($P_b$) is defined as the length of time expected from an investment to recover its initial cost in terms of profit or savings and it can be calculated (Sreekumar *et al.*, 2008).

$$P_b = \frac{\ln\left[1 - \frac{C_c}{S_1}\left(R_s - R_i\right)\right]}{\ln\left(\frac{1+R_i}{1+R_s}\right)} \tag{22}$$

$$P_b = \frac{\ln(0.704109589)}{\ln(0.944954128)} = 6.19\ Years \tag{23}$$

**Where:**

$C_c$ is the capital cost = TZS 1 800 000

$S_1$ is solar dryer savings for first year = TZS 365 000

$R_s$ is the rate of interest = 9% or 0.09

$R_i$ is the rate of inflation =3% or 0.03

Therefore, Payback ($P_b$) is equal to 6.2 years.

The economic analysis presented in this study it can be used to evaluate the financial feasibility of a solar dryer integrated with a heat storage system. Table 3 sets out the values of the different input parameters and the cost estimates of the components used in the design of the solar dryer integrated with the heat storage system and financial assessment. Due to the extra cost of drying food products and crops by using passive solar dryers and open sun drying system, there is an option of improving drying period, efficiency and quality of food products by integrating the solar dryer with other systems that can store energy for later use.

The economic evaluation was conducted using a payback period method to understand whether the technology is economically feasible and accessible or not. The total cost of the solar dryer, integrated with heat energy storage system, was calculated as TZS 1 800 000, while the manufacturing cost of the solar dryer without heat storage system was nearly half of a system's total cost. The solar dryer's life span has been estimated to be 22 years, while the payback period has been discovered to be 6.2 years, this is small compared to the lifespan of the 22-year solar dryer as payback computed using Equation (23) in Chapter 3.

# CHAPTER FIVE

# CONCLUSION AND RECOMMENDATIONS

## 5.1 Conclusion

The solar dryer, integrated with heat energy storage system, was successfully designed, manufactured and tested under no-load and load conditions, resulting in a maximum drying temperature of 62.4°C and averaging 46°C in sunny and cloudy days. The nitrate salt as a heat storage medium is extremely useful for drying food products in the current research because it can store heat to be used at a subsequent moment when sunlight is not active. Furthermore, open sun drying has been performed with respect to solar dryer drying which reduced the original moisture content from 86% (w.b) to the desired 10% (w.b) for 24 hours compared to 36 hours of drying in the sun. The advanced system's economic assessment was also conducted through a payback period of 6.2 years, which is low compared to the 22-year solar dryer life.

## 5.2 Recommendations

Further studies are still needed to design and modify the solar dryer, integrated with heat storage devices to preserve more heat storage to be used for lengthy periods of missing sunlight. The structure also needed a powerful insulation in the future research to minimize heat loss.

It is also suggested that further study may be carried out on other heat storage materials that have phased change characteristics that can store thermal energy at lower or higher temperatures.

## REFERENCES


Alamu, O. J., Nwaokocha, C. N., & Adunola, O. (2010). Design and construction of a domestic passive solar food dryer. *Leonardo Journal of Sciences,*16, 71-82.

Alimohammadi, Z., Akhijahani, H. S., & Salami, P. (2020). Thermal analysis of a solar dryer equipped with PTSC and PCM using experimental and numerical methods. *Solar Energy*, 201, 157-177.

Atalay, H. (2019). Performance analysis of a solar dryer integrated with the packed bed thermal energy storage system. *Energy*, 172, 1037-1052.

Azaizia, Z., Kooli, S., Hamdi, I., Elkhal, W., & Guizani, A.A. (2020). Experimental study of a new mixed mode solar greenhouse drying system with and without thermal energy storage for pepper. *Renewable Energy*, 145,1972-1984.

Bahari, M., Najafi, B., & Babapoor, A. (2020). Evaluation of α-AL2O3-PW nanocomposites for thermal energy storage in the agro-products solar dryer. *Journal of Energy Storage*, 28, 1-9.

Bakari, R., Minja, R. J., & Njau, K. N. (2014). Effect of glass thickness on performance of flat plate solar collectors for fruits drying, *Journal of Energy*, 2014, 1-9

Bellos, E., Tzivanidis, C., Antonopoulos, K., & Gkinis, G. (2016). Thermal enhancement of solar parabolic trough collectors by using nanofluids and converging-diverging absorber tube. *Renewable Energy*, 94, 213-222.

Bhardwaj, A., Kumar, R., & Chauhan, R. (2019). Experimental investigation of the performance of a novel solar dryer for drying medicinal plants in Western Himalayan region. *Solar Energy*, 177, 395-407.

Blomley, T., & Ramadhani, H. (2006). Going to scale with participatory forest management: Early lessons from Tanzania. *International Forestry Review*, 8(1), 93-100.

César, L. V. E., Lilia, C. M. A., Octavio, G. V., Isaac, P. F., & Rogelio, B. O. (2020). Thermal performance of a passive, mixed-type solar dryer for tomato slices (*Solanum lycopersicum*). *Renewable Energy*, 147, 845-855.

Chavan, A., Vitankar, V., Mujumdar, A., & Thorat, B. (2020). Natural convection and direct type (NCDT) solar dryers: A review. *Drying Technology*, 39(13),1-22.

Comission, C. C. A. (2003). *General Principles of Food Hygiene, CAC/RCP 1 - 1969 Rev.4*: *Codex Alimentarius Comission (pp. 1 - 31)*. https://www.google.com

Conrado, L. S., Rodriguez-Pulido, A., & Calderón, G. (2017). Thermal performance of parabolic trough solar collectors. *Renewable and Sustainable Energy Reviews,* 67, 1345-1359.

Da Cunha, J. P., & Eames, P. (2016). Thermal energy storage for low and medium temperature applications using phase change materials: A review. *Applied Energy*, 177, 227-238.

Ellabban, O., Abu-Rub, H., & Blaabjerg, F. (2014). Renewable energy resources: Current status, future prospects and their enabling technology. *Renewable and Sustainable Energy Reviews*, 39, 748-764.

Fterich, M., Chouikhi, H., Bentaher, H., & Maalej, A. (2018). Experimental parametric study of a mixed-mode forced convection solar dryer equipped with a PV/T air collector. *Solar Energy*, 171, 751-760.

Fudholi, A., Sopian, K., Gabbasa, M., Bakhtyar, B., Yahya, M., Ruslan, M. H., & Mat, S. (2015). Techno-economic of solar drying systems with water based solar collectors in Malaysia: A review. *Renewable and Sustainable Energy Reviews*, 51, 809-820.

Gabisa, E.W., & Aman, A. (2016). Characterization and experimental investigation of $NaNO_3$: $KNO_3$ as solar thermal energy storage for potential cooking application. *Journal of Solar Energy Engineering*, 2016.

Gulcimen, F., Karakaya, H., & Durmus, A. (2016). Drying of sweet basil with solar air collectors. *Renewable Energy*, 93, 77-86.

Hafez, A., Attia, A., Eltwab, H., ElKousy, A., Afifi, A., Abd-Elhamid, A., Abd-Elqader, A., Fateen, S. K., El-Metwally, K., & Soliman, A. (2018). Design analysis of solar parabolic trough thermal collectors. *Renewable and Sustainable Energy Reviews*, 82, 1215-1260.

Hussein, J., Hassan, M., Kareem, S., & Filli, K. (2017). Design, construction and testing of a hybrid photovoltaic (PV) solar dryer. *Environment*, 1(5), 1-14.

Ismaeel, H. H., & Yumrutaş, R. (2020). Thermal performance of a solar-assisted heat pump drying system with thermal energy storage tank and heat recovery unit. *International Journal of Energy Research*, 44(5), 3426-3445.

Jain, D., & Tewari, P. (2015). Performance of indirect through pass natural convective solar crop dryer with phase change thermal energy storage. *Renewable Energy*, 80, 244-250.

Joardder, M., Halder, P., Rahim, M., & Masud, M. (2017). *Solar pyrolysis: Converting waste into asset using solar energy, Clean Energy for Sustainable Development*. https://www.google.com

Kalbande, S., Jadhav, P., Khambalkar, V., & Deshmukh, S. (2017). Design of solar dryer assisted with reflector for drying of medicinal crops. *International Journal of Current Microbiology and Applied Sciences*, 6(2), 170-184.

Kant, K., Shukla, A., & Sharma, A. (2017). Advancement in phase change materials for thermal energy storage applications. *Solar Energy Materials and Solar Cells*, 172, 82-92.

Karthikeyan, R., Kumar, R. A., Manikandan, P., & Senthilnathan, A. (2021). Investigation of solar air heater with phase change materials using packed bed absorber plate. *Materials Today: Proceedings*, 45, 1360-1365.

Kondareddy, R., Sivakumaran, N., Radhakrishnan, K., & Nayak, P. K. (Eds.) (2020). *Performance analysis of solar tunnel dryer with thermal storage and Photovoltaic system for drying star fruit*. https://www.google.com

Lamrani, B., & Draoui, A. (2020). Thermal performance and economic analysis of an indirect solar dryer of wood integrated with packed-bed thermal energy storage system: A case study of solar thermal applications. *Drying Technology*, 1-18.

Lingayat, A., Chandramohan, V., & Raju, V. (2017). Design, development and performance of indirect type solar dryer for banana drying. *Energy Procedia*, 109, 409-416.

Lingayat, A. B., Chandramohan, V., Raju, V., & Meda, V. (2020). A review on indirect type solar dryers for agricultural crops: Dryer setup, its performance, energy storage and important highlights. *Applied Energy*, 258, 1-22.

Lu, W., Liu, G., Xiong, Z., Wu, Z., & Zhang, G. (2020). An experimental investigation of composite phase change materials of ternary nitrate and expanded graphite for medium-temperature thermal energy storage. *Solar Energy*, 195, 573-580.

Mawire, A., Lentswe, K., Owusu, P., Shobo, A., Darkwa, J., Calautit, J., & Worall, M. (2020). Performance comparison of two solar cooking storage pots combined with wonderbag slow cookers for off-sunshine cooking. *Solar Energy*, 208, 1166-1180.

Mehta, P., Samaddar, S., Patel, P., Markam, B., & Maiti, S. (2018). Design and performance analysis of a mixed mode tent-type solar dryer for fish-drying in coastal areas. *Solar Energy*, 170, 671-681.

Mohamed, F. M., Jassim, A. S., Mahmood, Y. H., & Ahmed, M. A. (2012). Design and study of portable solar dish concentrator. *International Journal of Recent Research and Review*, 3, 52-59.

Mohamed, S. A., Al-Sulaiman, F. A., Ibrahim, N. I., Zahir, M. H., Al-Ahmed, A., Saidur, R., Yılbaş, B., & Sahin, A. (2017). A review on current status and challenges of inorganic phase change materials for thermal energy storage systems. *Renewable and Sustainable Energy Reviews*, 70, 1072-1089.

Mongi, R. J., Ndabikunze, B. K., Wicklund, T., Chove, L. M., & Chove, B. E. (2015). Effect of solar drying methods on total phenolic contents and antioxidant activity of commonly consumed fruits and vegetable (mango, banana, pineapple and tomato) in Tanzania. *African Journal of Food Science*, 9(5), 291-300.

Mustayen, A., Mekhilef, S., & Saidur, R. (2014). Performance study of different solar dryers: A review. *Renewable and Sustainable Energy Reviews*, 34, 463-470.

Ndukwu, M., Onyenwigwe, D., Abam, F., Eke, A., & Dirioha, C. (2020). Development of a low-cost wind-powered active solar dryer integrated with glycerol as thermal storage. *Renewable Energy*, 154, 553-568.

Nimrotham, C., Songprakorp, R., Thepa, S., & Monyakul, V. (2017). Experimental research of drying red chili by two methods: Solar drying and low-temperature system drying. *Energy Procedia*, 138, 512-517.

Pankaew, P., Aumporn, O., Janjai, S., Pattarapanitchai, S., Sangsan, M., & Bala, B. (2020). Performance of a large-scale greenhouse solar dryer integrated with phase change material thermal storage system for drying of chili. *International Journal of Green Energy*, 17(11), 632-643.

Panwar, N., Kaushik, S., & Kothari, S. (2011). Solar greenhouse an option for renewable and sustainable farming. *Renewable and Sustainable Energy Reviews*, 15(8), 3934-3945.

Poblete, R., & Painemal, O. (2020). Improvement of the solar drying process of sludge using thermal storage. *Journal of Environmental Management*, 1(255), 1-8.

Rabha, D., & Muthukumar, P. (2017). Performance studies on a forced convection solar dryer integrated with a paraffin wax–based latent heat storage system. *Solar Energy*, 149, 214-226.

Rosli, M. I., Mu'im-Abdul-Nasir, A., Takriff, M. S., & Ravichandar, V. (2020). Drying sago pith waste in a fluidized bed dryer. *Food and Bioproducts Processing*, 123, 335-344.

Scanlin, D. (1997). *Indirect, through-pass, solar food dryer. Home Power. February*. https://www.google.com

Şevik, S., Aktaş, M., Dolgun, E. C., Arslan, E., & Tuncer, A. D. (2019). Performance analysis of solar and solar-infrared dryer of mint and apple slices using energy-exergy methodology. *Solar Energy*, 180, 537-549.

Sreekumar, A., Manikantan, P., & Vijayakumar, K. (2008). Performance of indirect solar cabinet dryer. *Energy Conversion and Management*, 49(6), 1388-1395.

Suleiman, R. A., & Kurt, R. A. (Eds.) (2015). *Current maize production, postharvest losses and the risk of mycotoxins contamination in Tanzania*. https://www.google.com

Tomar, V., Tiwari, G., & Norton, B. (2017). Solar dryers for tropical food preservation: Thermophysics of crops, systems and components. *Solar Energy*. 154, 2-13.

Tuncer, A. D., Sözen, A., Khanlari, A., Amini, A., & Şirin, C. (2020). Thermal performance analysis of a quadruple-pass solar air collector assisted pilot-scale greenhouse dryer. *Solar Energy*, 203, 304-316.

Ugwuoke, I. C., Ikechukwu, I. B., & Ifianyi, O. E. (2019). Design and development of a mixed-mode domestic solar dryer. *International Journal of Engineering and Manufacturing,* 9(3), 55-65.

Wang, W., Li, M., Hassanien, R. H. E., Wang, Y., & Yang, L. (2018). Thermal performance of indirect forced convection solar dryer and kinetics analysis of mango. *Applied Thermal Engineering*, 134, 310-321.

Yadav, S., & Chandramohan, V. (2020). Performance comparison of thermal energy storage system for indirect solar dryer with and without finned copper tube. *Sustainable Energy Technologies and Assessments*, 37, 100609.

Zhang, H., Baeyens, J., Cáceres, G., Degreve, J., & Lv, Y. (2016). Thermal energy storage: Recent developments and practical aspects. *Progress in Energy and Combustion Science*, 53, 1-40.

# APPENDICES

## Appendix 1: Solar dish collector

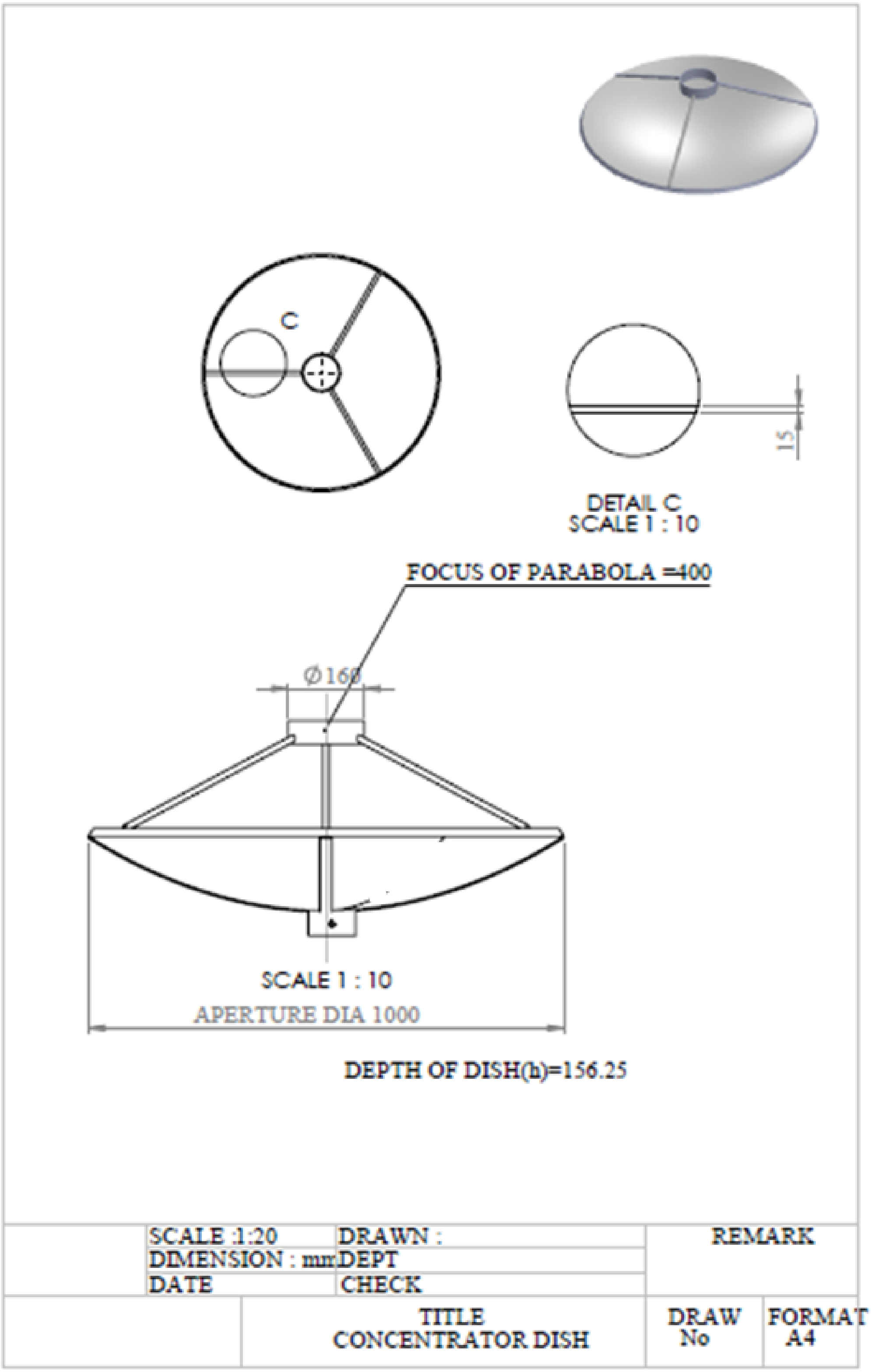

**Appendix 2: Cavity receiver**

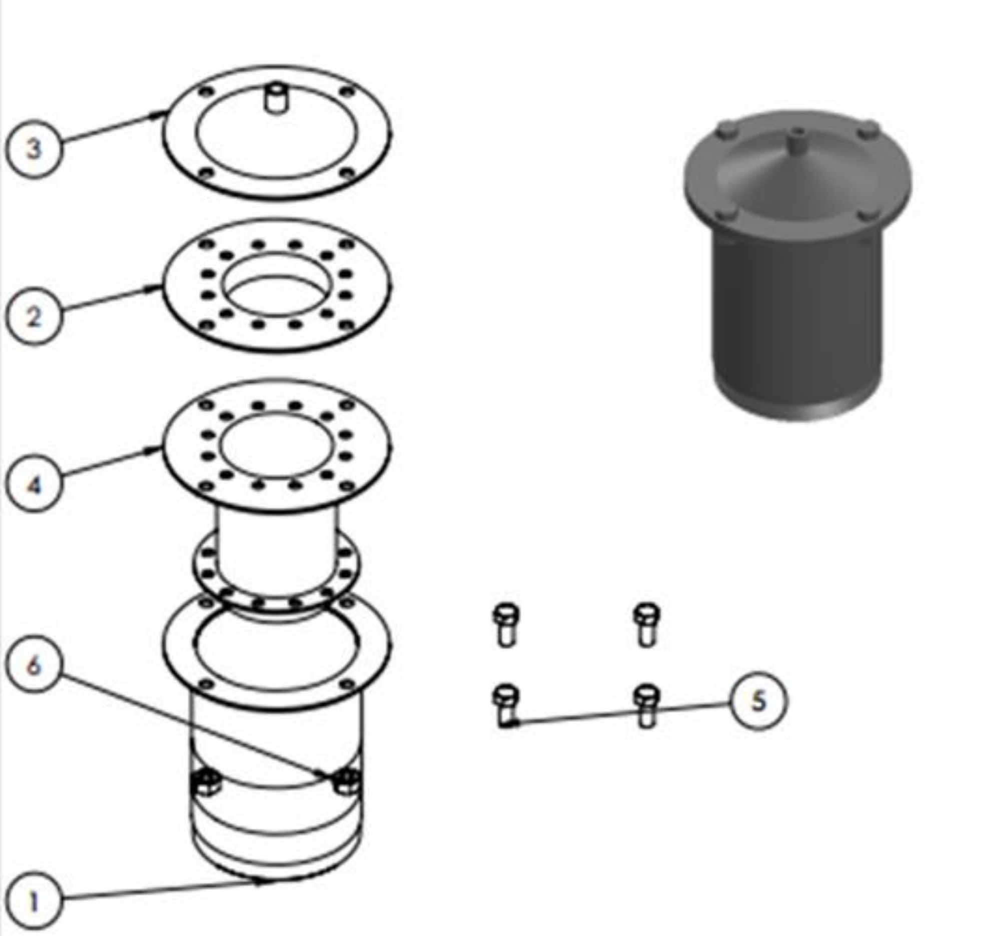


| ITEM NO. | PART NUMBER | DESCRIPTION | QTY. |
|---|---|---|---|
| 1 | ENCLOSURE | | 1 |
| 2 | Part3 | | 1 |
| 3 | Part4 | | 1 |
| 4 | PRT 2 | | 1 |
| 5 | B18.6.7M - M12 x 1.75 x 25 Plain HHMS --25C | | 4 |
| 6 | B18.2.4.6M - Heavy hex nut, M12 x 1.75 --W-N | | 4 |

| | | |
|---|---|---|
| SCALE : | DRAWN : | REMARK |
| DIMENSION : mm | DEPT | |
| DATE | CHECK | |

| | | |
|---|---|---|
| TITLE CAVITY RECEIVER | DRAW No | FORMAT A4 |

# Appendix 3: Solar dryer assembly

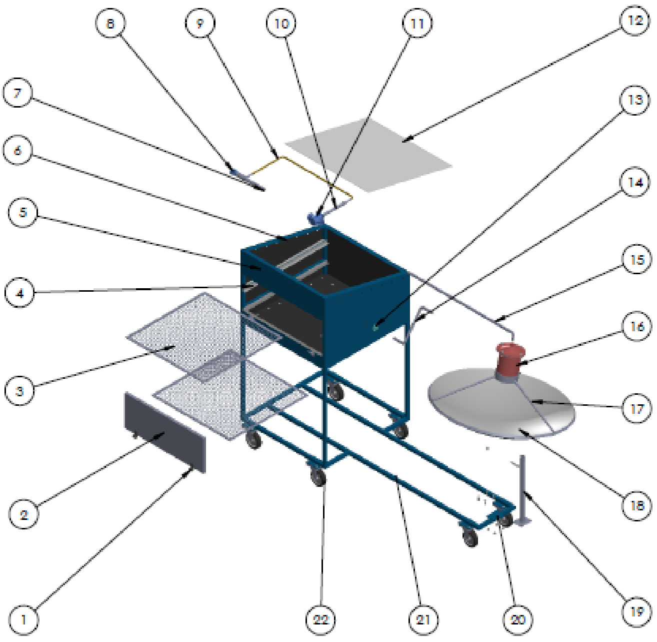


| PART NO. | ITEM | DESCRIPTION | QTY |
|---|---|---|---|
| 1 | HINGE | | 2 |
| 2 | DOOR | | 1 |
| 3 | TRAY | WIRE MESH | 2 |
| 4 | RAIL | | 4 |
| 5 | DRYER | | 1 |
| 6 | AIR VENT | HOLES | 44 |
| 7 | SENSOR | | 1 |
| 8 | KNOB | | 1 |
| 9 | CAPILLARY TUBE | | 1 |
| 10 | ACTUATOR | | 1 |
| 11 | VALVE | 2 WAY PORT | 1 |
| 12 | SOLAR COLLECTOR | TLANSPARENT GLASS | 1 |
| 13 | COUPLING | | 1 |
| 14 | CONNECTING PIPE | | 1 |
| 15 | TRANSMISSION PIPE | | 1 |
| 16 | CAVITY RECEIVER | | 1 |
| 17 | SUPPORTING BAR | | 3 |
| 18 | SOLAR DISH | | 1 |
| 19 | DISH STAND | | 1 |
| 20 | MOUNTING PLATE | | 1 |
| 21 | MAIN STAND | | 1 |
| 22 | CASTOR WHEEL | | 6 |

DRYER ASSEMBLY

A3

**Appendix 4: Data of ambient temperature**

| Time (Hrs) | Ambient temp (°C) Day 1 | Ambient temp (°C) Day 2 | Ambient temp (°C) Day 3 | Ambient temp (°C) Day 4 | Ambient temp (°C) Day 5 | Ambient temp (°C) Day 6 |
|---|---|---|---|---|---|---|
| 9:00 | 22.8 | 20.2 | 22.2 | 25.2 | 27.9 | 21.3 |
| 9:30 | 23.9 | 23.6 | 24 | 28.3 | 28.3 | 23.2 |
| 10:00 | 23.9 | 23.3 | 25.2 | 29.6 | 30.2 | 24.5 |
| 10:30 | 28.6 | 24.3 | 27.2 | 26.7 | 29.7 | 26.3 |
| 11:00 | 32.2 | 26.8 | 27 | 31.3 | 32.3 | 28 |
| 11:30 | 32.2 | 27.3 | 32 | 35.2 | 29.7 | 28.4 |
| 12:00 | 27 | 27.5 | 33.6 | 33.3 | 32.6 | 30.7 |
| 12:30 | 29.6 | 32.6 | 28.1 | 29.9 | 33.5 | 30.4 |
| 13:00 | 25.2 | 28.7 | 29 | 30.5 | 29.6 | 31.4 |
| 13:30 | 27.6 | 28.6 | 30.4 | 31.8 | 30.2 | 28.2 |
| 14:00 | 27.1 | 27.7 | 30.4 | 31.1 | 30.2 | 29.7 |
| 14:30 | 26.6 | 28.5 | 30.5 | 31.8 | 32.9 | 30.1 |
| 15:00 | 29.3 | 29 | 29.4 | 32.9 | 30.8 | 31 |
| 15:30 | 26.3 | 30.5 | 29.2 | 33.5 | 29.8 | 28.3 |
| 16:00 | 28.3 | 31 | 29 | 31.1 | 30.5 | 28.9 |
| 16:30 | 27.2 | 28.3 | 32.9 | 29.8 | 31.9 | 29.6 |
| 17:00 | 29.3 | 28.1 | 35.4 | 29.1 | 29.4 | 29.5 |
| 17:30 | 25.6 | 29.7 | 32.7 | 30.6 | 28.6 | 30.1 |
| 18:00 | 24.8 | 27.2 | 28.9 | 28 | 27.1 | 27.9 |
| 18:30 | 22.7 | 24.9 | 25.6 | 25.6 | 25.3 | 25.6 |
| 19:00 | 21.7 | 23.2 | 23 | 23.9 | 24.4 | 24.6 |
| 19:30 | 19.8 | 22.4 | 22.2 | 23.3 | 23.4 | 23.5 |
| 20:00 | 19.4 | 21.6 | 21.6 | 22.7 | 23.2 | 22.8 |
| 20:30 | 19.9 | 22.6 | 21.4 | 22.5 | 22.7 | 22.2 |
| 21:00 | 20.1 | 22.4 | 21.4 | 22.4 | 22.7 | 21.7 |

**Appendix 5: Data of relative humidity**

| Time (Hrs) | Relative humidity (% rh)<br><br>Day 1 | Relative humidity (% rh)<br><br>Day 2 | Relative humidity (% rh)<br><br>Day 3 | Relative humidity (% rh)<br><br>Day 4 | Relative humidity (% rh)<br><br>Day 5 | Relative humidity (% rh)<br><br>Day 6 |
|---|---|---|---|---|---|---|
| 9:00 | 66.9 | 72.3 | 66.6 | 61.7 | 55.2 | 77.8 |
| 9:30 | 61.7 | 59.9 | 60.6 | 53.1 | 54.3 | 72.8 |
| 10:00 | 60.8 | 58.6 | 57 | 48.2 | 49.4 | 67 |
| 10:30 | 46.8 | 57.5 | 53.5 | 54.2 | 52.6 | 59.9 |
| 11:00 | 37.9 | 50.7 | 53.1 | 42.8 | 41.8 | 51 |
| 11:30 | 36.8 | 46.2 | 41 | 36.2 | 44.2 | 51.3 |
| 12:00 | 46.6 | 46.4 | 39.4 | 38.4 | 39.8 | 44.5 |
| 12:30 | 43.3 | 40 | 48 | 44.3 | 37.5 | 44.3 |
| 13:00 | 50.5 | 43.9 | 46 | 42.9 | 43.4 | 40.3 |
| 13:30 | 46.4 | 43.2 | 43.3 | 40.9 | 40.2 | 45.5 |
| 14:00 | 46.8 | 43.8 | 43.7 | 39.3 | 42.1 | 42.7 |
| 14:30 | 46.9 | 42.5 | 43 | 38.4 | 37.3 | 40.2 |
| 15:00 | 40.4 | 41.2 | 42.6 | 35.8 | 38.1 | 41 |
| 15:30 | 47 | 38.2 | 41.5 | 31.7 | 40.7 | 43.1 |
| 16:00 | 41.8 | 37.5 | 42.3 | 35.8 | 37.5 | 41.8 |
| 16:30 | 42.3 | 40.8 | 35.1 | 38.7 | 36.8 | 41.2 |
| 17:00 | 37.9 | 41.5 | 31.2 | 41.2 | 45.7 | 39.4 |
| 17:30 | 46.4 | 37.1 | 35.2 | 38.9 | 47 | 39.9 |
| 18:00 | 49.4 | 40.3 | 40.7 | 41.2 | 50.7 | 45.4 |
| 18:30 | 54.3 | 44.9 | 46.6 | 43.4 | 54.3 | 51.2 |
| 19:00 | 58.1 | 51.8 | 55.1 | 47.4 | 56.4 | 53.2 |
| 19:30 | 65.1 | 52.3 | 53.6 | 50.4 | 58.7 | 57 |
| 20:00 | 66.8 | 56.1 | 53.9 | 52 | 59.4 | 60 |
| 20:30 | 65.1 | 55 | 52.5 | 53.3 | 61.2 | 62.5 |
| 21:00 | 64.4 | 59.9 | 51.8 | 55 | 62 | 63.3 |

**Appendix 6: Data of solar radiation intensity**

| Time (Hrs) | Solar intensity (W/m²)<br><br>Day 1 | Solar intensity (W/m²)<br><br>Day 2 | Solar intensity (W/m²)<br><br>Day 3 | Solar intensity (W/m²)<br><br>Day 4 | Solar intensity (W/m²)<br><br>Day 5 | Solar intensity (W/m²)<br><br>Day 6 |
|---|---|---|---|---|---|---|
| 9:00 | 303 | 658 | 191.5 | 588 | 196.5 | 255 |
| 9:30 | 501 | 747 | 322 | 581 | 191.2 | 331 |
| 10:00 | 933 | 801 | 478 | 826 | 416 | 392 |
| 10:30 | 677 | 837 | 818 | 890 | 1040 | 545 |
| 11:00 | 347 | 942 | 815 | 1095 | 560 | 459 |
| 11:30 | 849 | 960 | 650 | 1031 | 1061 | 621 |
| 12:00 | 990 | 1018 | 688 | 850 | 552 | 857 |
| 12:30 | 579 | 994 | 976 | 942 | 1004 | 707 |
| 13:00 | 1327 | 1054 | 1124 | 261 | 1098 | 1259 |
| 13:30 | 1058 | 1120 | 1001 | 303 | 1047 | 931 |
| 14:00 | 903 | 1168 | 1061 | 963 | 985 | 212 |
| 14:30 | 1141 | 484 | 440 | 682 | 612 | 986 |
| 15:00 | 301 | 476 | 887 | 788 | 1036 | 407 |
| 15:30 | 897 | 444 | 802 | 786 | 210 | 328 |
| 16:00 | 683 | 353 | 719 | 467 | 77 | 289 |
| 16:30 | 661 | 204 | 612 | 249 | 73 | 106.6 |
| 17:00 | 361 | 494 | 74.2 | 38.1 | 14.7 | 18.8 |
| 17:30 | 199.2 | 205 | 81.3 | 19.4 | 16.2 | 14.5 |
| 18:00 | 44 | 48.2 | 47.5 | 9.6 | 1.5 | 10 |

**Appendix 7: Data of air-drying temperature without load test for 4 days**

| Time (Hrs) | Drying temp (°C) - day 1 | Drying temp (°C) - day 2 | Drying temp (°C) - day 3 | Drying temp (°C) - day 4 | Drying temp (°C) - Average of 4 days |
|---|---|---|---|---|---|
| 9:00 | 27.5 | 26.6 | 26.3 | 31.3 | 27.93 |
| 9:30 | 36.1 | 33.6 | 29.8 | 38.4 | 34.48 |
| 10:00 | 31.7 | 37.8 | 34.1 | 45.8 | 37.35 |
| 10:30 | 43.7 | 47.1 | 44.3 | 38.8 | 43.48 |
| 11:00 | 47.1 | 56.1 | 49.7 | 42.8 | 48.93 |
| 11:30 | 51.5 | 54.5 | 48 | 51.6 | 51.40 |
| 12:00 | 51.8 | 55.4 | 53.7 | 51.8 | 53.18 |
| 12:30 | 58.2 | 56.3 | 48.7 | 54.8 | 54.50 |
| 13:00 | 44.8 | 59.7 | 55.8 | 57.7 | 54.50 |
| 13:30 | 45.5 | 60.9 | 58.5 | 58.3 | 55.80 |
| 14:00 | 43.5 | 58.1 | 55.8 | 60.6 | 54.50 |
| 14:30 | 47.8 | 59.3 | 59.5 | 60.1 | 56.68 |
| 15:00 | 48.1 | 57.4 | 55.7 | 59.4 | 55.15 |
| 15:30 | 37.4 | 55.3 | 55.8 | 55.8 | 51.08 |
| 16:00 | 49.4 | 52.7 | 50.5 | 55.7 | 52.08 |
| 16:30 | 42.6 | 49.3 | 46.6 | 48.3 | 46.70 |
| 17:00 | 34.3 | 46 | 42 | 45.2 | 41.88 |
| 17:30 | 30 | 36.1 | 37.8 | 35.1 | 34.75 |
| 18:00 | 27.8 | 32.2 | 33.1 | 31.6 | 31.18 |
| 18:30 | 24.6 | 27.7 | 28.2 | 27.7 | 27.05 |
| 19:00 | 22.8 | 24.6 | 24.9 | 25 | 24.33 |
| 19:30 | 21.2 | 22.9 | 22.8 | 23.6 | 22.63 |
| 20:00 | 19.8 | 21.9 | 21.7 | 22.7 | 21.53 |
| 20:30 | 19.6 | 21.3 | 20.9 | 22.3 | 21.03 |
| 21:00 | 19.7 | 21.9 | 20.6 | 22 | 21.05 |

**Appendix 8: Data of heat storage medium temperature without load test (at top) for 4 days**

| Time (Hrs) | Heat storage medium temp (°C) at top - day 1 | Heat storage medium temp (°C) at top - day 2 | Heat storage medium temp (°C) at top - day 3 | Heat storage medium temp (°C) at top - day 4 | Heat storage medium temp (°C) at top - Average of 4 days |
|---|---|---|---|---|---|
| 9:00 | 18.3 | 19.5 | 19.6 | 22.3 | 19.93 |
| 9:30 | 19.3 | 20.2 | 21.3 | 27.5 | 22.08 |
| 10:00 | 21.5 | 21.4 | 24.8 | 36 | 25.93 |
| 10:30 | 25.2 | 23 | 29.5 | 48.3 | 31.50 |
| 11:00 | 31.3 | 26.7 | 31.6 | 61.1 | 37.68 |
| 11:30 | 39.8 | 37 | 33.6 | 70.8 | 45.30 |
| 12:00 | 49.4 | 49.1 | 41.7 | 75.7 | 53.98 |
| 12:30 | 61.6 | 60.7 | 55.4 | 76.8 | 63.63 |
| 13:00 | 71.7 | 68.2 | 67.6 | 78.3 | 71.45 |
| 13:30 | 77.3 | 72.5 | 75 | 79.5 | 76.08 |
| 14:00 | 78.7 | 75.5 | 78.8 | 78.4 | 77.85 |
| 14:30 | 78.6 | 78.6 | 82.1 | 71.7 | 77.75 |
| 15:00 | 78.9 | 82.9 | 84.3 | 62.4 | 77.13 |
| 15:30 | 80.4 | 85.2 | 87 | 53.7 | 76.58 |
| 16:00 | 81.5 | 86.3 | 87.8 | 46.8 | 75.60 |
| 16:30 | 79.7 | 84.7 | 86.3 | 41.9 | 73.15 |
| 17:00 | 74.7 | 80.1 | 81.7 | 38.5 | 68.75 |
| 17:30 | 67.8 | 74.8 | 74.8 | 35.9 | 63.33 |
| 18:00 | 61 | 69.1 | 67.8 | 34 | 57.98 |
| 18:30 | 55.2 | 63 | 61 | 32.3 | 52.88 |
| 19:00 | 50.1 | 56.9 | 54.6 | 30.4 | 48.00 |
| 19:30 | 45.8 | 51.3 | 49.3 | 28.9 | 43.83 |
| 20:00 | 41.9 | 46.3 | 44.5 | 27.5 | 40.05 |
| 20:30 | 38.5 | 42.1 | 40.5 | 26.2 | 36.83 |
| 21:00 | 35.5 | 38.5 | 37.2 | 25.1 | 34.08 |

**Appendix 9: Data of heat storage medium temperature without load test (at bottom) for 4 days**

| Time (Hrs) | HSM temp (°C) at bottom - day 1 | HSM temp (°C) at bottom - day 2 | HSM temp (°C) at bottom - day 3 | HSM temp (°C) at bottom - day 4 | HSM temp (°C) at bottom –Av. of 4 days |
|---|---|---|---|---|---|
| 9:00 | 24 | 28.1 | 22.6 | 41.6 | 29.08 |
| 9:30 | 38.8 | 97.7 | 25 | 99.2 | 65.18 |
| 10:00 | 96.3 | 125 | 33.6 | 122 | 94.23 |
| 10:30 | 125 | 125 | 51.5 | 125 | 106.63 |
| 11:00 | 100.1 | 125 | 125 | 125 | 118.78 |
| 11:30 | 86.7 | 125 | 125 | 125 | 115.43 |
| 12:00 | 100.3 | 125 | 125 | 125 | 118.83 |
| 12:30 | 125 | 125 | 125 | 125 | 125.00 |
| 13:00 | 99.3 | 125 | 125 | 125 | 118.58 |
| 13:30 | 120.9 | 125 | 125 | 104.1 | 118.75 |
| 14:00 | 125 | 125 | 125 | 125 | 125.00 |
| 14:30 | 125 | 109.1 | 125 | 125 | 121.03 |
| 15:00 | 125 | 101.4 | 125 | 125 | 119.10 |
| 15:30 | 103.3 | 80.3 | 125 | 119.6 | 107.05 |
| 16:00 | 120.5 | 73.1 | 125 | 110.9 | 107.38 |
| 16:30 | 105.5 | 60.4 | 118.5 | 88.1 | 93.13 |
| 17:00 | 83.2 | 52.9 | 93.5 | 74.2 | 75.95 |
| 17:30 | 69.9 | 47.7 | 79.4 | 65 | 65.50 |
| 18:00 | 61.4 | 44.3 | 69.8 | 57.8 | 58.33 |
| 18:30 | 54.6 | 41.4 | 62.3 | 51.6 | 52.48 |
| 19:00 | 49 | 38.6 | 55.4 | 46.4 | 47.35 |
| 19:30 | 44 | 36 | 49.6 | 42 | 42.90 |
| 20:00 | 39.8 | 33.7 | 44.7 | 38.3 | 39.13 |
| 20:30 | 36.5 | 31.6 | 40.7 | 35.2 | 36.00 |
| 21:00 | 33.6 | 29.7 | 37.5 | 32.8 | 33.40 |

**Appendix 10: Data of air drying with load drying test for 2 days**

| Time (Hrs) | Drying temp (°C) - day 1 | Drying temp (°C) - day 2 | Drying temp (°C) -Average of 2 days |
|---|---|---|---|
| 9:00 | 40.7 | 45.5 | 43.10 |
| 9:30 | 41 | 53.3 | 47.15 |
| 10:00 | 46.2 | 60.9 | 53.55 |
| 10:30 | 46.2 | 60.8 | 53.50 |
| 11:00 | 51.2 | 57.5 | 54.35 |
| 11:30 | 53.2 | 54.8 | 54.00 |
| 12:00 | 51.7 | 57 | 54.35 |
| 12:30 | 48.3 | 52.3 | 50.30 |
| 13:00 | 55.1 | 60.4 | 57.75 |
| 13:30 | 57.6 | 55.2 | 56.40 |
| 14:00 | 57 | 58.8 | 57.90 |
| 14:30 | 60.1 | 58.8 | 59.45 |
| 15:00 | 58.2 | 54 | 56.10 |
| 15:30 | 43.8 | 52 | 47.90 |
| 16:00 | 44.4 | 48 | 46.20 |
| 16:30 | 48.5 | 41.9 | 45.20 |
| 17:00 | 35.3 | 33.6 | 34.45 |
| 17:30 | 32.5 | 30.8 | 31.65 |
| 18:00 | 29.5 | 29.2 | 29.35 |
| 18:30 | 26.5 | 26.7 | 26.60 |
| 19:00 | 25 | 24.9 | 24.95 |
| 19:30 | 23.8 | 24.1 | 23.95 |
| 20:00 | 23.2 | 23.9 | 23.55 |
| 20:30 | 22.8 | 23.6 | 23.20 |
| 21:00 | 22.3 | 22.6 | 22.45 |

**Appendix 11: Data of heat storage medium temperature for load drying test (at top) for 2 days**

| Time (Hrs) | Heat storage medium temp (°C) at top - day 1 | Heat storage medium temp (°C) at top - day 2 | Heat storage medium temp (°C) at top -Average of 2 days |
|---|---|---|---|
| 9:00 | 20.6 | 22.3 | 21.45 |
| 9:30 | 21.4 | 27.5 | 24.45 |
| 10:00 | 23.5 | 36 | 29.75 |
| 10:30 | 25.5 | 48.3 | 36.90 |
| 11:00 | 31.7 | 61.1 | 46.40 |
| 11:30 | 44.5 | 70.8 | 57.65 |
| 12:00 | 61.8 | 75.7 | 68.75 |
| 12:30 | 81 | 76.8 | 78.90 |
| 13:00 | 90 | 78.3 | 84.15 |
| 13:30 | 92.8 | 79.5 | 86.15 |
| 14:00 | 89.5 | 78.4 | 83.95 |
| 14:30 | 97.1 | 71.7 | 84.40 |
| 15:00 | 92.9 | 62.4 | 77.65 |
| 15:30 | 91 | 53.7 | 72.35 |
| 16:00 | 85.3 | 46.8 | 66.05 |
| 16:30 | 76 | 41.9 | 58.95 |
| 17:00 | 66.7 | 38.5 | 52.60 |
| 17:30 | 58.7 | 35.9 | 47.30 |
| 18:00 | 52.2 | 34 | 43.10 |
| 18:30 | 47.1 | 32.3 | 39.70 |
| 19:00 | 42.9 | 30.4 | 36.65 |
| 19:30 | 39.2 | 28.9 | 34.05 |
| 20:00 | 36.3 | 27.5 | 31.90 |
| 20:30 | 33.8 | 26.2 | 30.00 |
| 21:00 | 31.8 | 25.1 | 28.45 |

**Appendix 12: Data of heat storage medium temperature for load drying test (at bottom) for 2 days**

| Time (Hrs) | Heat storage medium temp (°C) at bottom - day 1 | Heat storage medium temp (°C) at bottom - day 2 | Heat storage medium temp (°C) at bottom - Average of 2 days |
|---|---|---|---|
| 9:00 | 22 | 22.2 | 22.10 |
| 9:30 | 23.5 | 29 | 26.25 |
| 10:00 | 26.5 | 36.4 | 31.45 |
| 10:30 | 48.8 | 53 | 50.90 |
| 11:00 | 124 | 45.8 | 84.90 |
| 11:30 | 125 | 68.6 | 96.80 |
| 12:00 | 125 | 77.7 | 101.35 |
| 12:30 | 104.8 | 114.1 | 109.45 |
| 13:00 | 113 | 125 | 119.00 |
| 13:30 | 125 | 125 | 125.00 |
| 14:00 | 115.8 | 125 | 120.40 |
| 14:30 | 80.2 | 119.8 | 100.00 |
| 15:00 | 63.4 | 125 | 94.20 |
| 15:30 | 51 | 89.8 | 70.40 |
| 16:00 | 40.2 | 71.9 | 56.05 |
| 16:30 | 34.4 | 59.3 | 46.85 |
| 17:00 | 29.7 | 52.2 | 40.95 |
| 17:30 | 27.2 | 47.3 | 37.25 |
| 18:00 | 26.1 | 43.5 | 34.80 |
| 18:30 | 25.2 | 40.4 | 32.80 |
| 19:00 | 24 | 37.8 | 30.90 |
| 19:30 | 22.6 | 35.5 | 29.05 |
| 20:00 | 21.5 | 33.6 | 27.55 |
| 20:30 | 20.4 | 31.8 | 26.10 |
| 21:00 | 19.7 | 30.2 | 24.95 |

## Appendix 13: Data of moisture content with load drying test for solar dryer and sun drying systems

| Drying time (hrs) | Time (hour) | Solar dryer drying (w.b %) | Open sun drying (w.b %) |
|---|---|---|---|
| -Day 1 | 9:00 | 86 | 86 |
| 1 | 10:00 | 81.1 | 82.5 |
| 2 | 11:00 | 72.5 | 78.2 |
| 3 | 12:00 | 63 | 73 |
| 4 | 13:00 | 55 | 68.5 |
| 5 | 14:00 | 46.5 | 65.8 |
| 6 | 15:00 | 37.5 | 61.5 |
| 7 | 16:00 | 30.6 | 58.5 |
| 8 | 17:00 | 26.5 | 56.5 |
| 9 | 18:00 | 25.3 | 55.8 |
| 10 | 19:00 | 24.7 | 55 |
| 11 | 20:00 | 24.6 | 54.4 |
| 12 | 21:00 | 24.5 | 54.2 |
| -Day 2 | 9:00 | 24.5 | 54.2 |
| 13 | 10:00 | 23.1 | 53.5 |
| 14 | 11:00 | 18.7 | 49.1 |
| 15 | 12:00 | 17.7 | 46.5 |
| 16 | 13:00 | 15.4 | 45.9 |
| 17 | 14:00 | 14.6 | 44 |
| 18 | 15:00 | 13.6 | 41.2 |
| 19 | 16:00 | 12.5 | 38.6 |
| 20 | 17:00 | 11.3 | 35 |
| 21 | 18:00 | 11 | 30.6 |
| 22 | 19:00 | 10.8 | 27.6 |
| 23 | 20:00 | 10.2 | 26.3 |
| 24 | 21:00 | 10 | 23.7 |
| -Day 3 | 9:00 | | 23.7 |
| 25 | 10:00 | | 21.3 |
| 26 | 11:00 | | 20.6 |
| 27 | 12:00 | | 18.2 |
| 28 | 13:00 | | 16.6 |
| 29 | 14:00 | | 14.6 |
| 30 | 15:00 | | 13.4 |
| 31 | 16:00 | | 12.9 |
| 32 | 17:00 | | 12.4 |
| 33 | 18:00 | | 12 |
| 34 | 19:00 | | 11.6 |

**Appendix 14: Photography of solar dryer, integrated with heat energy storage system**

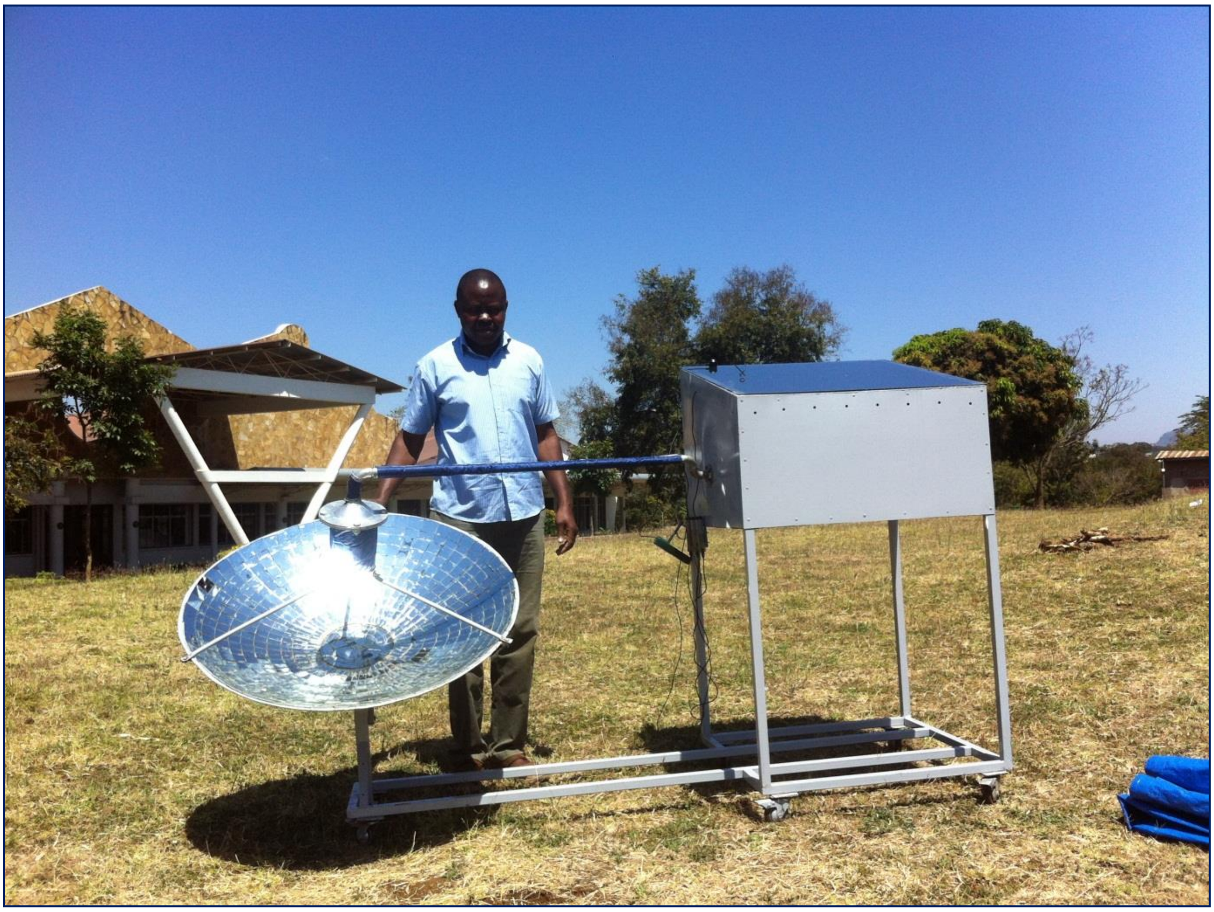

## Appendix 15: Drying of red peppers

## RESEARCH OUTPUTS

### Output 1: Research Article

Missana, W. P., Park, E., & Kivevele, T. T. (2020). Thermal Performance Analysis of Solar Dryer Integrated with Heat Energy Storage System and a Low-Cost Parabolic Solar Dish Concentrator for Food Preservation. *Journal of Energy*, 2020, 1-10.

### Output 2: Poster Presentation

Hindawi
Journal of Energy
Volume 2020, Article ID 9205283, 10 pages
https://doi.org/10.1155/2020/9205283

*Research Article*

# Thermal Performance Analysis of Solar Dryer Integrated with Heat Energy Storage System and a Low-Cost Parabolic Solar Dish Concentrator for Food Preservation

**Wenceslaus Pantaleo Missana**,[1,2] **Eugene Park**,[1] **and Thomas T. Kivevele**[1]

[1]*Department of Materials and Energy Science and Engineering, Nelson Mandela African Institution of Science and Technology (NM-AIST), P. O. Box, 447 Arusha, Tanzania*
[2]*Department of Automotive Engineering, Arusha Technical College (ATC), P. O. Box, 296 Arusha, Tanzania*

Correspondence should be addressed to Wenceslaus Pantaleo Missana; missanaw@nm-aist.ac.tz

Received 8 February 2020; Revised 20 June 2020; Accepted 13 July 2020; Published 30 July 2020

Academic Editor: Hao Wu



Solar energy has become a viable alternative energy because it is a clean type of energy that converts solar radiation into heat energy for various applications such as heating water, power generation, cooking, and food drying. The solar dryer, integrated with the heat energy storage system, uses nitrate salt as a heat storage medium which was designed and tested by drying 1000 grams of red pepper at 19.6 to 62.4°C. The average ambient temperature ranged from 19.3 to 37.4°C, and the maximum temperature of the heat storage media ranged from 87.8 to 125°C. The solar drying process was compared to open sun drying system loaded with 1000 grams of red pepper. The findings showed that the solar dryer maintained color and flavor and lowered the original moisture content from 86% to 10% for 24 hours compared to 36 hours of drying in open air. In this study, nitrate salt is shown to be the perfect heat storage medium for drying food products; it preserved heat for about 4 hours when there is no active sunlight.

## 1. Introduction

Solar energy transforms solar radiation into heat energy to dry food and plants [1]. In many nations, agricultural products, particularly vegetables and fruits, are lost for over 40% of postharvest through spoilage [2]. It is therefore inevitable that solar dryers are used for dry agricultural products, as discussed in [3].

The common drying systems are open sun and controlled solar dryer. Open sun drying is a common way to preserve food that involves putting crops on mats, roofs, or drying floors in the sun and is an inexpensive way to dry out. However, due to dust, dirt, fungi, bacteria, and animal attacks, the product may be spoiled as studied in [4]. The controlled drying system involves the use of active and passive solar dryers as described in [5]. Thus, the active solar dryer is an efficient solar dryer used in small firms for drying products for a brief time period, but the technology is still expensive for farmers as discussed in [6]. Likewise, the passive solar dryer is commonly used because it is an inexpensive technology, but the dryer fails to operate when there is no active sunlight. It is therefore essential to integrate a thermal storage system into the solar dryers, which can allow heat collection during sunlight to be used later when there is no sunlight, thus improving efficiency as presented in [7]. Many recent studies investigate solar dryers that integrated with heat storage systems using different techniques. For instance, [8] investigated indirect forced convection solar dryer integrated with SHSM and PCM; the scrap of iron combined with gravel and the engine oil in the solar air collector was used as SHSM and the rt-42 paraffin was used as a PCM. The drying rate for SHSM and PCM was 0.051 kg/hr; SHSM's energy and exergy efficiency was 26.1 and 0.81%, respectively, moisture content decreased from an initial value of 89% to 9%. Reference [9] studied mixed-mode forced convection solar dryer and assessed thermal photovoltaic air in the air collector and drying room. The air surrounding the PV panels cooled the PV cells and supplied thermal energy to the drying chamber. The moisture content of the product decreased from 91.94 to 22.32% for tray 1 and to 28.9% for tray 2 with a difference of 6.6%. Reference [10] described the indirect forced convection solar dryer for mango drying testing. The specific rate of moisture extraction was 1.67 kg/kWh at a drying temperature of 52°C, and the average thermal efficiency ranged from 30.9 to 33.8%. Reference [11] developed an indirect type solar dryer to study banana's drying characteristics The moisture content of bananas decreased from the initial value of 356% in dry basis to the final moisture content of 16.3%, 19.5%, 21.2%, 31.2%, and 42.4% for tray 1, tray 2, tray 3, tray 4, and open sun drying, respectively. The collector's average thermal efficiency was 31.5%, and that of the drying chamber was 22.4%. Reference [12] designed a greenhouse solar dryer; the tests for drying takes 52 hours to reduce the moisture content from 74% to 13.5% (w.b). The average of air-drying temperature and relative humidity reached to 50°C and 36% RH, respectively. Reference [13] reviewed some studies of solar dryer based on thermal energy storage materials and described that it was quite efficient in continually drying agriculture and food products with temperatures from 40°C and 60°C. Reference [14] researched solar thermal energy storage for cooking application. 1.4 kg PCM charged up to 300°C for 50 minutes, while discharged from 300°C to 100°C for 4.5 hours. As discussed, $NaNO_3$ (60%) : $KNO_3$ (40%) were the appropriate choice for potential cooking by storing the cheapest solar thermal energy and good thermal characteristics.

Several researches addressed the poor performance of passive solar dyers compared to those combined with the heat storage system. Thus, further studies are needed to design solar dryers, which are incorporated with heat storage systems to preserve more heat that can be used in the absence of active sunlight. The combination of potassium nitrate ($KNO_3$ (40%)) and sodium nitrate ($NaNO_3$ (60%)) known as a nitrate salt is a good example of heat storage material that has excellent thermal properties as assessed [14]. These chemical compounds have not been used as heat storage medium in solar dryers. Most of the studies have used it for power generation and cooking applications. Carefully, this study found its performance as a heat storage medium used in a solar dryer integrated with heat storage system. The solar dryer was constructed and integrated with a low-cost solar dish concentrator to maximize the collection of solar energy and store it in the thermal storage materials used when sunlight is not present.

## 2. Materials and Methods

*2.1. Materials.* The following materials were used and sold on the local market for the construction of the solar dryer: square pipes and sheets, stainless steel pipes and sheets, aluminum sheets, angle iron, and clear transparent glass.

*2.2. Designing of a Solar Dryer.* The solar dryer, integrated with the heat energy storage system, was developed and tested. The construction took place in three steps, starting with the drying chamber, solar dish collector with sun-tracking system, and cavity receiver, and then, it was placed along the*N*-*S*axis in the study area to track the sun for experimentation. The drying chamber's overall dimensions were about 0.8 m × 0.8 m × 0.4 (width, length, and depth), inclined to support the solar collector at an angle of 13.3995°. Inside the drying chamber were fitted two grilled trays of 0.06 m diameter to support the drying products. Due to pressure difference, the air temperature was recalculated by natural convection, so that the temperature inside the drying chamber is constant to prevent vacuum formation inside the solar dryer. In order to enable air circulation, 0.07 m diameter holes were drilled at the base side and around the top of the drying chamber.

Solar collector inclination angle ($\beta$) from horizontal position was calculated using the following formula [15]:

$$\beta = 10^\circ + \text{latitude}\theta, \tag{1}$$

where the study area's latitude $\theta$ is equal to 3.3995° S.

Therefore, the collector inclination angle is equal to 10° + 3.3995° S = 13.3995°.

The solar collector's thermal energy can be defined as [16]

$$Energy_{\text{input}} = \text{Energy}_{\text{output}} + \text{Energy}_{\text{loss}}, \tag{2}$$

where

$\text{Energy}_{\text{loss}}$ is losses in thermal energy.

The energy gain from radiation by air can be found using the following equation:

$$\text{Energy}_{\text{gain}} = I_c A_c \eta_c, \tag{3}$$

where $I_c$ is the insolation at the collector surface in watt per square meter; $A_c$ is the area of the collector in square meter; and $\eta_c$ is the collector efficiency.

The collector efficiency can be found through the following equation:

$$\eta_c = \frac{\text{Energy}_{\text{gain}}}{I_c A_c}. \tag{4}$$

The total energy transmission and absorption are defined by the following equation:

$$I_c A_c \tau\alpha = \text{Energy}_{\text{gain}} + \text{Energy}_{\text{loss}}, \tag{5}$$

where $\tau$ is the transmissivity and $\alpha$ is the absorptivity.

*2.3. Parabolic Geometry.* The solar dish was designed by considering a locus of points that lie on equal distance from a line (directrix) and a point (focus) as shown in Figure 1. The fixed line is called a directory, and focus *F* is the fixed point. The perpendicular line to the directory that passed through focus *F* is known as the parabolic axis. The vertex intersects the parabolic dish at point *V* which is exactly the centre or midway [16].

The concentration ratio refers straight to the reflector's performance. If the origin is taken along the parabola axis

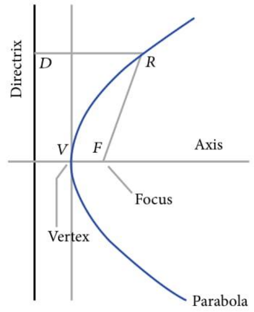


FIGURE 1: Parabolic geometry.

at the vertex $V$ and the $x$-axis, the parabola equation is given by

$$y^2 = 4fx. \tag{6}$$

When the origin of the coordinate is moved to point $F$ with the vertex to the left of the origin, the parabola equation becomes

$$y^2 = 4f(x + f), \tag{7}$$

where $f$ is focal length.

In polar coordinates, $r$ is the distance from the origin and $\theta$ is the angle from the $x$-axis to $r$ at the origin; the parabola can be determined with the following formula:

$$\frac{\sin^2\theta}{\cos\theta} = \frac{4f}{r}. \tag{8}$$

When an angle $\Psi$ is measured between $V$-$F$ and the radius of the parabolic $p$ which is the distance from the focal point $F$ to the parabolic curve, the following formula is required:

$$p = \frac{2f}{1 + \cos\psi_{\text{rim}}}. \tag{9}$$

The geometric concentration ratio ($CR_g$) is defined as the ratio of aperture area of the parabolic dish ($A_a$) to the receiver base area ($A_r$), and it is given by

$$CR_g = \frac{A_a}{A_r}, \tag{10}$$

where the aperture area of the parabolic dish can be determined by the following equation:

$$A_a = \frac{\pi}{4}(2p\sin\psi_{\text{rim}})^2. \tag{11}$$

By substituting $p$ from Equation (9), the aperture area of parabolic dish can be found using

$$A_a = 4\pi f^2 \frac{\sin^2\psi_{\text{rim}}}{(1 + \cos\psi_{\text{rim}})^2}. \tag{12}$$

By Snell's law the incidence angle is equal to the angle of reflection. The quantity of solar radiation intensity that comes parallel to the parabola's surface reflected back to the focus. So, the reflection angle is expressed as

$$\psi = 2p. \tag{13}$$

Rim angle $\Psi_{\text{rim}}$ represents the ratio of the focal length ($f$) to dish diameter or aperture width ($d$). For typical parabola, the depth of the curve ($H$) is measured from top to the bottom of the curve which is sometimes called the parabola height or depth. The focal length is measured from the focus ($F$) to the vertex ($V$); $h$ and $f$ are calculated by the following equations:

$$\begin{aligned} H &= \frac{d^2}{16f}, \\ H &= 0.15625\,\text{m}, \\ f &= \frac{d^2}{16H} \\ f &= 0.4\,m. \end{aligned} \tag{14}$$

Rim angle is the sole diameter of the shape of a parabola that can have some influence on the concentration ratio ($f/d$)

$$\frac{f}{d} = \frac{1}{4\tan(\psi_{\text{rim}}/2)}. \tag{15}$$

The rim angle ($\Psi_{\text{rim}}$) can be calculated by the following equation:

$$\tan\psi_{\text{rim}} = \frac{1}{(d/8H) - (2H/d)}. \tag{16}$$

Therefore, rim angle $\Psi_{\text{rim}} = 63.9°$.

Arc length ($s$) of the parabola is another important property of the parabola used when designing the solar concentrator and is calculated by the following formula:

$$S = \left[\frac{d}{2}\sqrt{\left(\frac{4H}{d}\right)^2 + 1}\right] + 2f\ln\left[\frac{4H}{d}\sqrt{\left(\frac{4H}{d}\right)^{-2} + 1}\right]. \tag{17}$$

The parabolic dish surface area can be given using the following equation:

$$A_{sc} = \frac{8\pi f^2}{3}\left[\left(\left[\frac{d}{4f}\right]^2 + 1\right)^{\frac{3}{2}} - 1\right]. \tag{18}$$

The energy input of the solar thermal collector can be determined by using

$$E_i = I_t A_{sc}. \tag{19}$$

The energy output of the solar thermal collector can be obtained using the following equation:

$$E_o = \frac{mC_p \Delta T}{t}. \tag{20}$$

The efficiency of the solar thermal collector can be defined as the ratio between the useful outputs of energy to the input energy as shown in

$$\eta = \left(\frac{E_o}{E_i}\right) 100\%. \tag{21}$$

The size of the curve was specified in linear dimension by looking at the focus point ($f$), rim angle ($\Psi_{rim}$), and aperture diameter ($d$). The segment of a parabola shared a focal point with the same aperture width giving a different rim angle with respect to the parabolic height as shown in Figure 2 and discussed in [17].

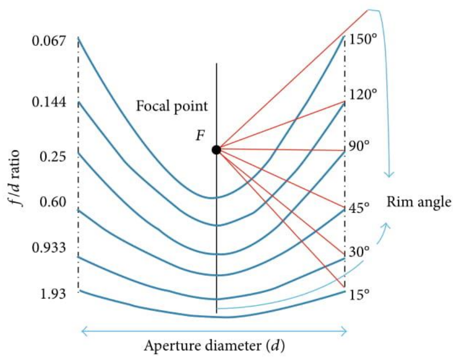


FIGURE 2: A segment of a parabola having a common focus point and rim angle with the same aperture diameter.

*2.3.1. Design Parameters and Dimensions of the Solar Parabolic Dish Concentrator.* Table 1 summarizes all important design parameters of the parabolic solar dish concentrator such as aperture diameter, focal length, concentrator depth, vertex, and rim angle.

TABLE 1: Design parameters of the solar parabolic dish concentrator.

| S/No. | Parameters | Numerical value | Unit |
|---|---|---|---|
| 1 | Aperture diameter ($d_a$) | 1 | M |
| 2 | Focal length ($f$) | 0.4 | M |
| 3 | Depth of the concentrator ($H$) | 0.15625 | M |
| 4 | Vertex ($V$) = $d/2$ | 0.5 | M |
| 5 | Rim angle ($\Psi_{rim}$) | 63.9 | ° |
| 6 | $f/d$ | 0.4 | — |

*2.3.2. Cavity Receiver.* The cavity receiver is the component used to correct the maximum quantity of solar radiation that was reflected back to the focal point with a heat source acting parabolic dish concentration as described in [18]. The cavity receiver was made of stainless-steel plate and cylindrical pipe of 2 mm thickness, coated with a thin layer of gray paint, and it was placed at a focal point. The aperture of the receiver area was calculated using

$$A_r = \frac{\pi}{4} d_r^2, \qquad A_r = 0.008107\ \text{m}^2. \tag{22}$$

*2.4. The Self-Acting Temperature Control.* The temperature required can be set on the knob connected to a temperature sensor and inserted into the drying chamber. As the temperature increases, the actuator automatically closes the valve, and if the temperature drops below the set temperature, the actuator automatically opens the valve. The temperature control valve comprises of a sensor, capillary tube, and actuator linked to the 2-port control valve. When a sensitive fluid is heated in the sensor and capillary tube, it will expand and contract when cooled. The force produced by the expansion or contraction is transferred via the capillary to the actuator to permit or stop the flow of hot air through the control valve. The adjustment knob is turned clockwise to decrease the set temperature, and vice versa to increase. Type SA121 (Spirax Sarco) was used to control heat from the storage system.

*2.5. Material for Heat Energy Storage.* Nitrate salt is used as a heat storage medium; the materials showed a good thermal characteristic and working temperature. Other factors such as storage duration, the temperature required, storage capacity, heat losses, economics, and space availability were also considered in selecting these materials. To utilize heat energy at least heat charging, heat storage and heat discharging should be achieved as shown in a flow diagram (Figure 3).

*2.6. Analyses*

*2.6.1. Error Analyses.* Errors occur due to difference between the actual value and the value indicated by the measuring instruments. During experimental analysis, temperature measurement, relative humidity, moisture loss, weight loss, solar intensity, and air velocity errors were undertaken via solar dryers integrated with heat energy storage system. In order to determine the total error in the measuring instruments, fixed, manufacture, and random errors were considered [19]. If $x$ represents the amount of error in each variable of the measurement, the total error can be found by

$$W_{th} = \left[(x_1)^2 + (x_2)^2 + \cdots (x_\infty)^2\right]^{1/2}. \tag{23}$$

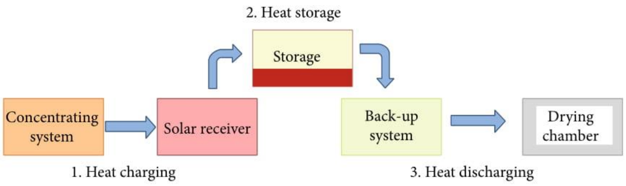


FIGURE 3: Utilization of heat energy.

TABLE 2: Total values of errors made in drying experiments.

| Instrument used | Parameter(s) causing error(s) | Unit | Total error |
|---|---|---|---|
| Data logger | Total error from heat (temperature) | | |
| | $W_{Ta}$—ambient temperature | °C | ±0.3 |
| | $W_{Tc}$—drying temperature | °C | ±0.3 |
| | $W_{Th}$—heat storage material temperature | °C | ±0.3 |
| Data logger | Total error from relative humidity | | |
| | $W_{Hr}$—relative humidity | % | ±3 |
| Digital balance scale | $W_M$—weight | g | ±0.01 |
| Solar power meter | $W_S$—solar radiation intensity | W/m$^2$ | ±10 |
| Anemometer | $W_V$—air velocity | m/s | ±0.104 |

Table 2 shows the total errors in measurement found in the solar dryer integrated with heat energy storage system.

*2.6.2. Efficiency Analyses.* A solar dryer integrated with heat energy storage system was used for the drying test in the experiment conducted. The following function expresses the change in air temperature ($\Delta T$) as [19]

$$(\Delta T) = f(I_c, A_c, \tau\alpha, E_i). \tag{24}$$

The useful energy used to determine the efficiency of the collector $Q_u$, can be calculated by using the following equation [19]:

$$Q_u = m\,C_p(T_o - T_i). \tag{25}$$

*2.6.3. Drying Analyses.* Moisture content can be described as the quantity of water in a wet sample as expressed in [20]. The moisture of the product relies on the situation of the environment, such as temperature and relative humidity, and can be expressed on a moist or dry basis. The amount of moisture to be removed from hot red peppers was calculated using Equation (25) as [8]

$$\mathrm{MC}_{wb} = \left[\frac{(M_t - M_f)}{M_t}\right] \times 100\%. \tag{26}$$

The drying rate is the amount of evaporated moisture per unit time and analyzes the system effectiveness that takes place during the drying period. Mathematically, it is calculated as

$$\mathrm{DR} = \frac{dM}{dt} = -k(M_t - M_e), \qquad \frac{dM}{(M_t - M_e)} = -k dt. \tag{27}$$

The moisture ratio was determined using the following equations:

$$\mathrm{MR} = \frac{(M_t - M_e)}{(M_i - M_e)}, \qquad \mathrm{MR} = \frac{M_t}{M_i}. \tag{28}$$

The formula used to determine the total amount of moisture to be removed, $M_w$, is expressed as

$$M_w = \frac{W_w = (M_i - M_f)}{1 - M_f}. \tag{29}$$

*2.7. Instrumentation and Measurement.* SNN–USB temperature/humidity data loggers with accuracy of ±0.3°C (±3%) and measurement ranges of -40 to 125° C (0 to 100% RH), respectively, were used to determine relative humidity and temperature at various places including ambient, air-drying, and thermal storage medium temperatures. After every two minutes, the readings were recorded from 9:00 to 21:00 hrs.

The solar power meter (TES-132 data logging) with a measuring range of 2000 W/m$^2$ and accuracy within ±10 W/m$^2$ or ± 5% was used to assess and to record the intensity of the solar radiation and was connected to the laptop.

*2.8. Experimental Procedure.* The solar dryer experiment was tested and compared in six scenarios: (i) solar dryer without load and heat storage system; (ii) solar dryer without load but with heat storage system; (iii) the combination of solar dryer and heat storage system without load; (iv) solar dryer with a load, but without a heat storage system; (v) solar dryer with load and heat storage system; and (vi) the combination of solar dryer and heat storage system with load. Red peppers were selected as sample biomaterial to be dried and assessed in this research as studied in [21]. Data measured were ambient, air-drying, and heat storage material temperature; relative humidity; and intensity of solar radiation. Using the oven drying technique, the original moisture content of red peppers was discovered as [12]. The sample was weighed using a USS–DBS2 digital analytical balance scale of measurement range 0-5000 g with an accuracy of ±0.01 g. One kg of red peppers was placed in a hot oven at 60°C for 12 hours; the initial moisture content was found to be 86% as evaluated in [22].

*2.9. Experimental Setup.* The experimental setup consisted of a parabolic solar dish collector, cavity receiver, temperature control system, glazing, drying chamber, and main frame. Nitrate salt was used as a heat storage medium and filled in the cavity receiver's internal cylinder (Figure 4).

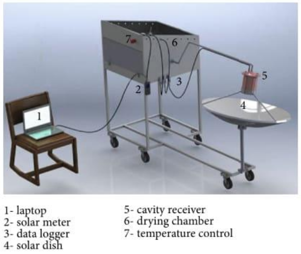


Figure 4: Schematic drawing of experimental setup.

## 3. Result and Discussion

The performance assessment of the solar dryer, integrated with heat energy storage system, was carried out in October 2018 in Arusha, Tanzania. The experiments were done every day for 12 hours from 9:00 to 21:00 for one week. During the experiments, the medium temperature for heat storage at most daylight hours was much greater than the temperature for ambient and air drying. Figure 5 shows results for variations in ambient air temperature with time, ranging from 19.3 to 37.4° C within days of experiments. The change of relative humidity of the atmospheric air was found to be between 28.3% and 77.8% as shown in Figure 6. During the experiment, the system was exposed to solar radiation for 6 days, the average solar radiation was 610.4 W/m$^2$ where the maximum solar intensity was 1327 W/m$^2$, and the parabolic solar dish collector was oriented and tracked manually when the sun moves in an interval of every 15 minutes (Figure 7).

*3.1. Solar Dryer without Load Tests.* Solar dryer without load tests were performed to assess the solar dryer without the application of a heat storage system; during the experiments, the temperature control valve was closed every day from 9:00 to 17:00 hours for four days without load tests. The average ambient air temperature was 27.7°C, while the maximum of air-drying temperature, heat storage medium, and solar intensity were 62.4°C, 125°C, and 1327 W/m$^2$, respectively. In the evening at 17:00 hours under no-load condition, the temperature control valve was opened to allow the application of a heat storage system; the maximum reading of air-drying temperature, heat storage medium, and solar intensity were found to be 46°C, 81.7°C, and 1259 W/m$^2$, respectively (Figure 8). As shown in Figure 9, the maximum heat storage medium temperature ranged from 87.8°C to 125°C. The weather was cloudy and sunny during the tests.

*3.2. Solar Dryer with Load Drying Tests.* The temperature control valve was closed during the daytime for load drying test without a heat storage system from 9:00 to 17:00 hours. The air ambient, air-drying, and heat storage medium temperature and solar intensity ranged from 21.3 to 33.5°C, 33.6 to 60.9°C, 20.6 to 125°C, and 44 to 1327 W/m$^2$, respectively. The air ambient, air-drying, and heat storage medium temperatures were slowly reduced from 33.5 to 21.7°C, 60.9 to 22.3°C, and 125 to 25.1°C in the evening under load test from 17:00 to 21:00 hours as shown in Figure 10. The maximum heat storage medium temperature ranged from 81.7° C to 125° C as shown in Figure 11.

*3.3. Drying Experiments of Red Pepper.* For comparison studies between the solar dryer and sun drying, two kg of fresh red peppers was measured to be dried. The fresh red peppers were assessed for their moisture content which was found to be 86% (w.b). Thus, 1000 g of red peppers was dried in the solar dryer for 24 hours; within two days, the moisture content decreased to 10% (w.b). Likewise, open sun drying took 36 hours to decrease the moisture content from 1000 g to achieve 10% (w.b) within three days as shown in Figure 12 below. Figure 13 shows the appearance of fresh red peppers before drying (a), red peppers after solar drying (b), and red peppers after open sun drying (c). The findings showed that the dried one in the solar dryer was better preserved without losing nutrients, color, and flavor compared to the ones dried in the open sun.

## 4. Conclusions

The solar dryer, integrated with heat energy storage system, was successfully designed, manufactured, and tested under no-load and load conditions, resulting in a maximum drying temperature of 62.4°C and averaging 46°C in sunny and cloudy days. Furthermore, the solar drying process was compared to open sun drying system loaded

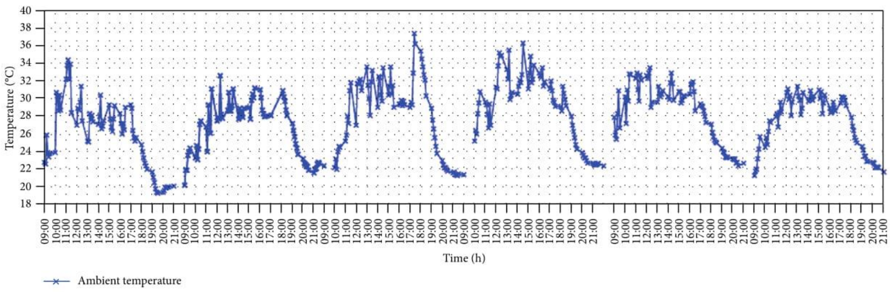


Figure 5: Variation of ambient temperature with time during the days of experiment.

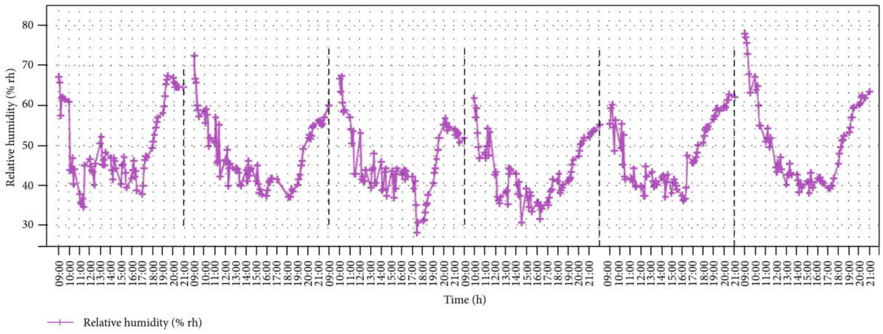


Figure 6: Variation of relative humidity with time during the days of experiment.

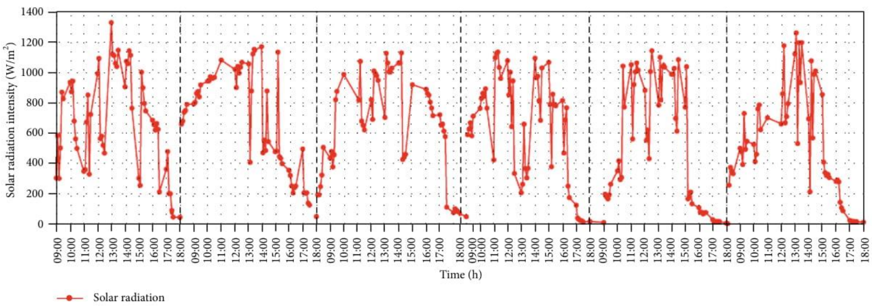


Figure 7: Variation of solar radiation intensity with time during the days of experiment.

with 1000 grams of red pepper. The findings showed that the solar dryer reduced its original moisture content from 86% to 10% for 24 hours, while the open sun drying took 36 hours to lower the same moisture content up to 10%. As a result of this study, nitrate salt as a heat storage medium was found to be highly beneficial for drying food products because it can store heat to be used at a later time when the sunlight is not active.

## 5. Recommendation

Further studies are still needed to design, fabricate, and evaluate the solar dryer, integrated with heat storage systems to preserve more heat storage to be used for lengthy periods of missing sunlight. The structure also needed a powerful insulation in the future research in order to minimize heat loss. It is also suggested that different scholars in the field of study

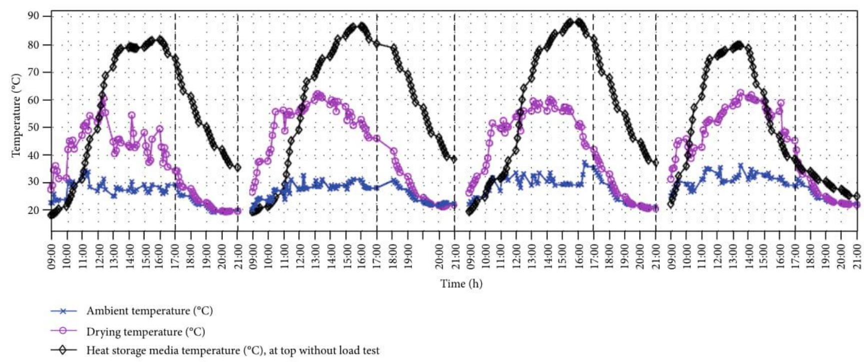


Figure 8: Variation of temperatures without load tests with time.

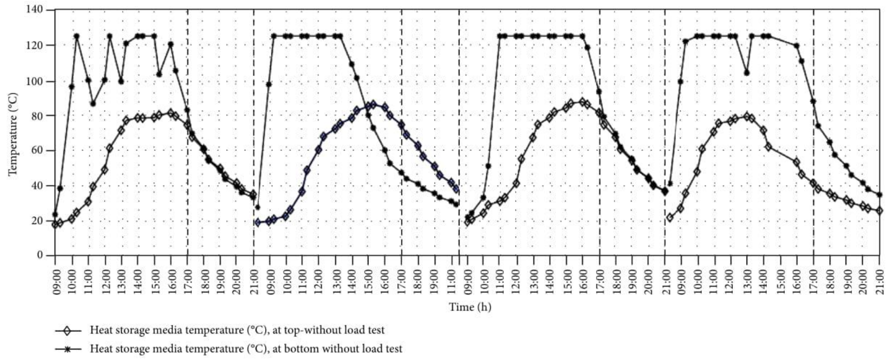


Figure 9: Variance of heat storage medium temperature without load tests at the top and bottom side with time.

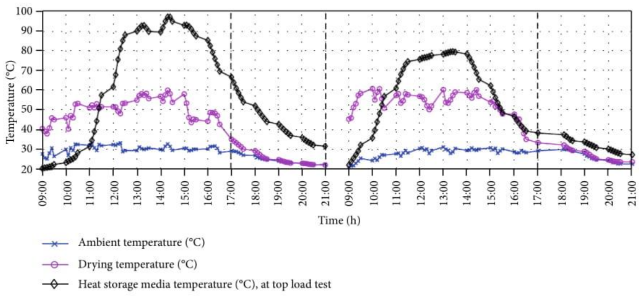


Figure 10: Variation of temperature of load drying tests with time.

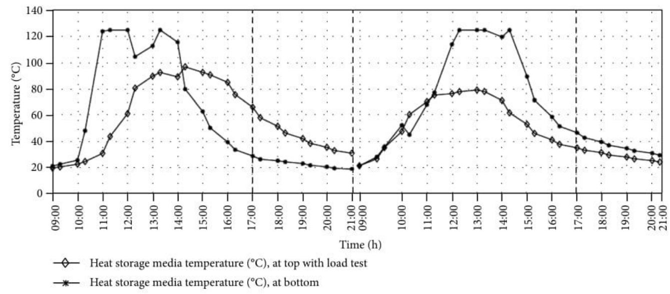


Figure 11: Variance of heat storage medium temperature of load drying tests on the top and bottom side with time.

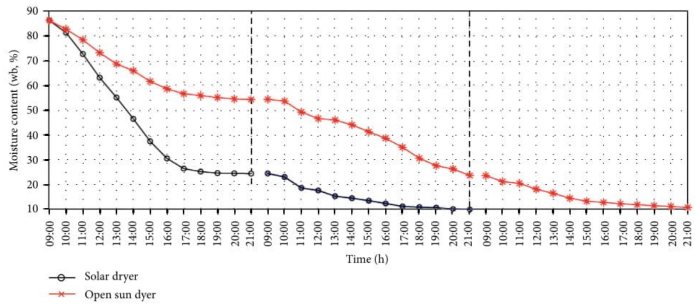


Figure 12: Variation of moisture content (w.b) of the solar dryer and open sun drying with drying time for red pepper samples.

(a) (b) (c)

Figure 13: (a) Fresh red peppers before drying. (b) Red peppers after solar drying. (c) Red peppers after open sun drying.

may investigate other heat storage materials based on phase change characteristics that can store thermal energy at lower and higher temperatures.

## Nomenclature

I: Solar intensity ($W/m^2$)
DR: Drying rate (kg of water/kg of dry matter per hour)
MR: Moisture ratio
$M$: Mass of product (kg)
MC: Moisture content (%)
$M_a$: Mass flow rate of air (kg/s)
$Cp_a$: Specific heat capacity of air (kj/kg K)
$\dot{Q}$: Heat transfer rate (W)
$T$: Temperature (°C)
$T$: Drying time (hour)
$V$: Velocity (m/s)
$CR_g$: Geometric concentration ratio
$F$: Focal length (m)
$D_a$: Aperture diameter (m)
$S$: Arc length of the parabolic curve (m)
$H$: Depth of parabola (m)
$E$: Energy (J)
$A_c$: Area of collector ($m^2$)
$A$: Area ($m^2$)
$Q$: Heat (W)
$NaNO_3$: Sodium nitrate
$KNO_3$: Potassium nitrate.

*Subscripts*

f: Final
i: Initial
w: Wet basis

c: Collector
e: Equilibrium.

*Greek symbols*

$\alpha$: Absorptivity
$\tau$: Transmissivity
$\eta$: Efficiency (%)
$\rho_a$: Density of air (kg/m$^3$)
$\psi$: Angle of reflection (°)
$\beta$: Angle of inclination (°)
$\phi$: Latitude (°)
$\Delta T$: Change in temperature (°C).

## Data Availability

We did not attach any information about data availability in our manuscript, but if required, will we send them.

## Conflicts of Interest

The authors declare that without any conflict of interest, this paper is being written and published.

## Acknowledgments

The authors acknowledge and express their sincere thanks to the Nelson Mandela African Institution of Science and Technology for supporting this study. Arusha Technical College and Higher Education Student's Loan Board of Tanzania funded this research work.

## References

[1] N. L. Panwar, S. C. Kaushik, and S. Kothari, "Role of renewable energy sources in environmental protection : a review," *Renewable and Sustainable Energy Reviews*, vol. 15, no. 3, pp. 1513–1524, 2011.

[2] R. A. Suleiman and K. A. Rosentrater, *Current maize production, postharvest losses and the risk of mycotoxins contamination in Tanzania*, 2015 ASABE Annual International Meeting (p. 1). American Society of Agricultural and Biological Engineers, 2015.

[3] S. R. Kalbande, P. Jadhav, V. P. Khambalkar, and S. Deshmukh, "Design of solar dryer assisted with reflector for drying of medicinal crops," *International Journal of Current Microbiology and Applied Sciences*, vol. 6, no. 2, pp. 170–184, 2017.

[4] M. Numbing and G. Maikasuwa, "Construction of domestic solar fish dryer," *Journal of Applied Physics*, vol. 7, no. 5, pp. 9–13, 2015.

[5] J. B. Hussein, M. A. Hassan, S. A. Kareem, and K. B. Filli, "Design , construction and testing of a hybrid photovoltaic (PV) solar dryer," *Environment*, vol. 1, no. 5, 2017.

[6] A. G. M. B. Mustayen, S. Mekhilef, and R. Saidur, "Performance study of different solar dryers: a review," *Renewable and Sustainable Energy Reviews*, vol. 34, pp. 463–470, 2014.

[7] W. Cheng, K. M. Sørensen, R. J. Mongi et al., "A comparative study of mango solar drying methods by visible and near-infrared spectroscopy coupled with ANOVA-simultaneous component analysis (ASCA)," *Lwt*, vol. 112, 2019.

[8] A. K. Bhardwaj, R. Kumar, and R. Chauhan, "Experimental investigation of the performance of a novel solar dryer for drying medicinal plants in Western Himalayan region," *Solar Energy*, vol. 177, pp. 395–407, 2019.

[9] M. Fterich, H. Chouikhi, H. Bentaher, and A. Maalej, "Experimental parametric study of a mixed-mode forced convection solar dryer equipped with a PV/T air collector," *Solar Energy*, vol. 171, pp. 751–760, 2018.

[10] W. Wang, M. Li, R. Hassanien, E. Hassanien, Y. Wang, and L. Yang, "Thermal performance of indirect forced convection solar dryer and kinetics analysis of mango," *Applied Thermal Engineering*, vol. 134, pp. 310–321, 2018.

[11] A. Lingayat, V. P. Chandramohan, and V. R. K. Raju, "Design, development and performance of indirect type solar dryer for banana drying," *Energy Procedia*, vol. 109, pp. 409–416, 2017.

[12] C. Nimrotham, R. Songprakorp, S. Thepa, and V. Monyakul, "Experimental research of drying red chili by two methods: solar drying and low - temperature system drying," *Energy Procedia*, vol. 138, pp. 512–517, 2017.

[13] K. Kant, A. Shukla, A. Sharma, A. Kumar, and A. Jain, "Thermal energy storage based solar drying systems: a review," *Innovative Food Science and Emerging Technologies*, vol. 34, pp. 86–99, 2016.

[14] E. W. Gabisa and A. Aman, "Characterization and experimental investigation of NaNO 3: KNO 3 as solar thermal energy storage for potential cooking application," *Journal of Solar Energy Engineering*, vol. 2016, article 2405094, 2016.

[15] J. A. Oguntola, N. N. Collins, and A. Olayinka, "Design and construction of a domestic passive solar food dryer," *Leonardo Journal of Sciences*, vol. 16, no. 16, pp. 71–82, 2010.

[16] F. M. Mohamed, A. S. Jassim, Y. H. Mahmood, and M. A. K. Ahmed, "Design and study of portable solar dish concentrator," *International Journal of Recent Research and Review*, vol. 3, pp. 52–59, 2012.

[17] H. Hijazi, O. Mokhiamar, and O. Elsamni, "Mechanical design of a low cost parabolic solar dish concentrator," *Alexandria Engineering Journal*, vol. 55, no. 1, pp. 1–11, 2016.

[18] A. M. Daabo, S. Mahmoud, and R. K. Al-dadah, "The effect of receiver geometry on the optical performance of a small-scale solar cavity receiver for parabolic dish applications," *Energy*, vol. 114, pp. 513–525, 2016.

[19] F. Gulcimen, H. Karakaya, and A. Durmus, "Drying of sweet basil with solar air collectors," *Renewable Energy*, vol. 93, pp. 77–86, 2016.

[20] A. ELkhadraoui, S. Kooli, I. Hamdi, and A. Farhat, "Experimental investigation and economic evaluation of a new mixed-mode solar greenhouse dryer for drying of red pepper and grape," *Renewable Energy*, vol. 77, pp. 1–8, 2015.

[21] D. K. Rabha and P. Muthukumar, "Performance studies on a forced convection solar dryer integrated with a paraffin wax–based latent heat storage system," *Solar Energy*, vol. 149, pp. 214–226, 2017.

[22] M. Madhava and A. R. Rao, "Drying of red chilli in photovoltaic powered greenhouse," *International Journal of Engineering Technology Science and Research*, vol. 4, no. 9, pp. 207–213, 2017.

## Output 2: Poster Presentation

# PERFORMANCE ASSESSMENT OF SOLAR DRYER INTEGRATED WITH HEAT ENERGY STORAGE SYSTEM FOR FOOD PRESERVATION

**Wenceslaus Pantaleo Missana, Dr. Thomas Kivevele**

*Department of Material, Energy Science and Engineering, NM-AIST, P. O. Box 447, Arusha – Tanzania*

### INTRODUCTION

Solar energy converts solar radiation into heat energy to dry food and plants. In many nations, agricultural products, particularly vegetables and fruits, are lost through spoilage. Therefore, using solar dryers to dry agricultural products is an economic way.

#### Research Objective

The main objective of the present study was to assess the performance of solar dryer, integrated with a heat storage system used nitrate salt as storage media for food preservation.

### MATERIALS AND METHODS

#### Materials

- Square pipes
- Angle iron
- Aluminum sheets
- Transparent clear glass
- Stainless steel pipes & sheets
- Nitrate salts

#### Methods

1. Experimental method
2. Oven drying method

#### Experimental set-up

### RESULTS AND DISCUSSION

The solar dryer, integrated with heat energy storage system, was tested by drying 1000g of red peppers in a drying air temperature range of 19.6 – 62.4°C while its average temperature was 46°C and ambient temperature ranges between 19.3 – 37.4°C. The drying process was compared with solar dryer and open sun drying system, each loaded with 1000g of red pepper, the solar dryer maintained colour, flavor and lowered the original moisture content by 86% to the required 10% for 24 hours, while the open sun drying took 36 hours to decrease the moisture content from 1000g to achieve the same amount.

#### Results

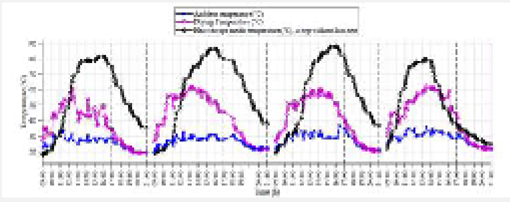

Fig.Temperature variation with time without load tests

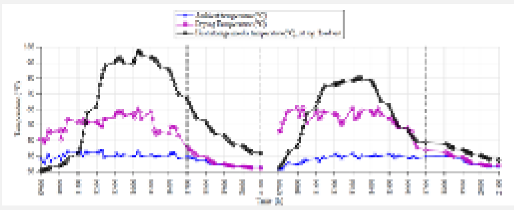

Fig.Temperature variation with time of load drying experiments

### CONCLUSION

As a result of this study, nitrate salt as a medium for heat storage is highly beneficial for drying food products because it can store heat to be used at a later time when sunlight is not active.